Southeastern Geology: Volume 49, No. 3
March 2013

Editor in Chief: S. Duncan Heron, Jr.

Abstract

Academic journal published quarterly by the Department of Geology, Duke University.

SOUTHEASTERN GEOLOGY

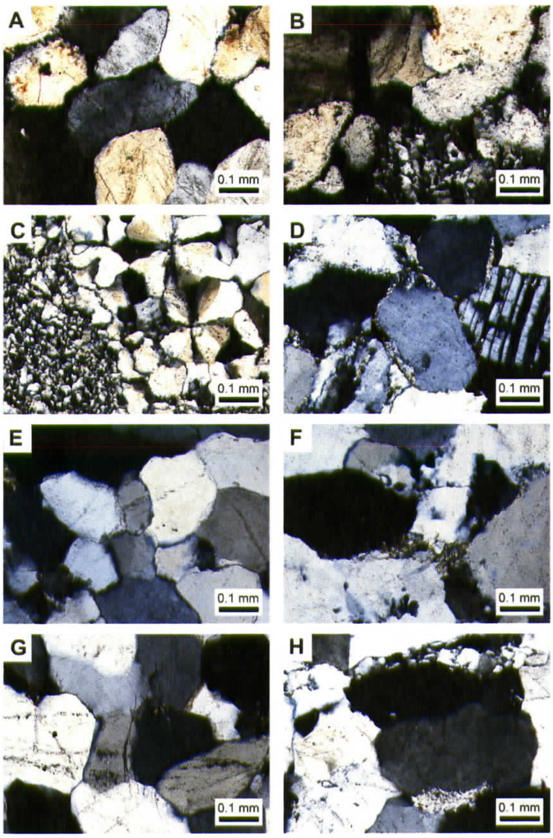

Vol. 49, No. 3

March 2013

SOUTHEASTERN GEOLOGY

PUBLISHED

at

UNIVERSITY OF WEST GEORGIA

This journal publishes the results of original research on all phases of geology, geophysics, geochemistry and environmental geology as related to the Southeast. Send manuscripts to **David Bush, Department of Geosciences, University of West Georgia, Carrollton, Georgia 30118, for Fed-X, etc. 1601 Maple St.,** Phone: 678-839-4057, Fax: 678-839-4071, Email: dbush@westga.edu. Please observe the following:

1) Type the manuscript with double space lines and submit in duplicate, or submit as an Acrobat file attached to an email.
2) Cite references and prepare bibliographic lists in accordance with the method found within the pages of this journal. Data citations examples can be found at http://www.geoinfo.org/TFGeosciData.htm
3) Submit line drawings and complex tables reduced to final publication size (no bigger than 8 x 5 3/8 inches, table text 8 pt Arial font).
4) Make certain that all photographs are sharp, clear, and of good contrast. Submit as jpeg quality 10 and pixel dimension at least 1600 for a landscape image.
5) Stratigraphic terminology should abide by the North American Stratigraphic Code (American Association Petroleum Geologists Bulletin, v. 67, p. 841-875).
6) Email Acrobat (pdf) submissions are encouraged.

Subscriptions to *Southeastern Geology* for volume 49 are: individuals - $28.00 (paid by personal check); corporations and libraries - $47.00; foreign $65. Inquiries should be sent to: **SOUTHEASTERN GEOLOGY, UNIVERSITY OF WEST GEORGIA, DEPARTMENT OF GEOSCIENCES, 1601 MAPLE STREET, CARROLLTON, GA 30118-0001**. Make checks payable to: *Southeastern Geology.*

Information about **SOUTHEASTERN GEOLOGY** is on the World Wide Web including a searchable author-title index 1958-2010 (Acrobat format). The URL for the Web site is: http://www.southeasterngeology.org

SOUTHEASTERN GEOLOGY is a peer review journal.

ISSN 0038-3678

SOUTHEASTERN GEOLOGY

Table of Contents

Volume 49, No. 3, March 2013

SOUTHEASTERN GEOLOGY
V. 49, No. 3, March 2013, p. 95-118

THE ORIGIN OF SANDSTONE XENOLITHS IN THE MOLE HILL BASALT, ROCKINGHAM COUNTY, VIRGINIA: IMPLICATIONS FOR MAGMA ASCENT AND CRUSTAL STRUCTURE IN THE WESTERN SHENANDOAH VALLEY

ELIZABETH A. JOHNSON[1], ZACHARY A. KIRACOFE[1], JOHN T. HAYNES[1], KANE NASHIMOTO[2]

[1]*Department of Geology and Environmental Science*
James Madison University
Harrisonburg, VA 22807
johns2ea@jmu.edu
[2]*Department of Mathematics and Statistics, James Madison University, Harrisonburg, VA 22807*

ABSTRACT

Mole Hill is an Eocene (48 Ma) basaltic volcanic neck located four miles west of Harrisonburg, in the Shenandoah Valley of Virginia. The basalt, which includes sandstone xenoliths and mantle-derived xenocrysts, exhibits moderate to poor columnar jointing in outcrop. Mole Hill is surrounded by a contact zone of hydrothermal chert formed through interaction of magmatic fluids with the limestone and dolostone of the Ordovician Beekmantown Formation. To constrain the origin of the sandstone xenoliths, petrographic and whole-rock geochemical analyses were obtained on samples of the sandstone xenoliths, the Mole Hill basalt, and regional sandstone units. Clast size (longest and shortest axes) and shape (long axis / short axis) were also measured for four of the sandstone xenoliths and five of the sandstone units. The xenoliths are clean white to tan sandstones in hand sample, and in thin section are comprised principally of monocrystalline quartz grains with minor polycrystalline quartz grains. The monocrystalline quartz grains contain linear to curvilinear tracks of fluid inclusions and have weak to moderate undulatory extinction. Optically continuous quartz overgrowths are present along the edges of some quartz grains, but the matrix and grain boundaries of the sandstone xenoliths were pervasively infiltrated by basaltic magma. A combination of textural evidence from hand samples and thin sections, clast size and shape, and a Principle Component Analysis (PCA) of the geochemical data indicate that the most likely source of the sandstone xenoliths at Mole Hill is the Silurian Tuscarora Formation, followed by the Devonian Oriskany Formation. Both the Tuscarora and Oriskany Formations are exposed along the NE-SW-striking North Mountain Fault Zone about 6 km to the west of Mole Hill. This implies that the basaltic magma of Mole Hill exploited splays and associated faults of the North Mountain thrust system as a conduit system for reaching the surface. The younger Silurian and Devonian rocks extend underneath Mole Hill and the Ordovician units of the western Shenandoah Valley in the footwall of the North Mountain Fault.

INTRODUCTION

Geology of Mole Hill

Mole Hill is an Eocene (48 Ma) basaltic volcanic neck located in Rockingham County, VA, 3 km west of the city of Harrisonburg (Figure 1; Wampler and Dooley, 1975; Southworth and others, 1993). It is the easternmost known body of a swarm of Eocene volcanic necks, dikes, and plugs exposed to the west and southwest in Pendleton County, WV, and Highland and Augusta Counties, VA (Southworth and others, 1993). The country rock surrounding the Mole Hill basalt is the limestone and dolostone of the Ordovician Beekmantown Formation (Gathright and Frischmann, 1986; Campbell and others, 2006). A vuggy chert is exposed in a

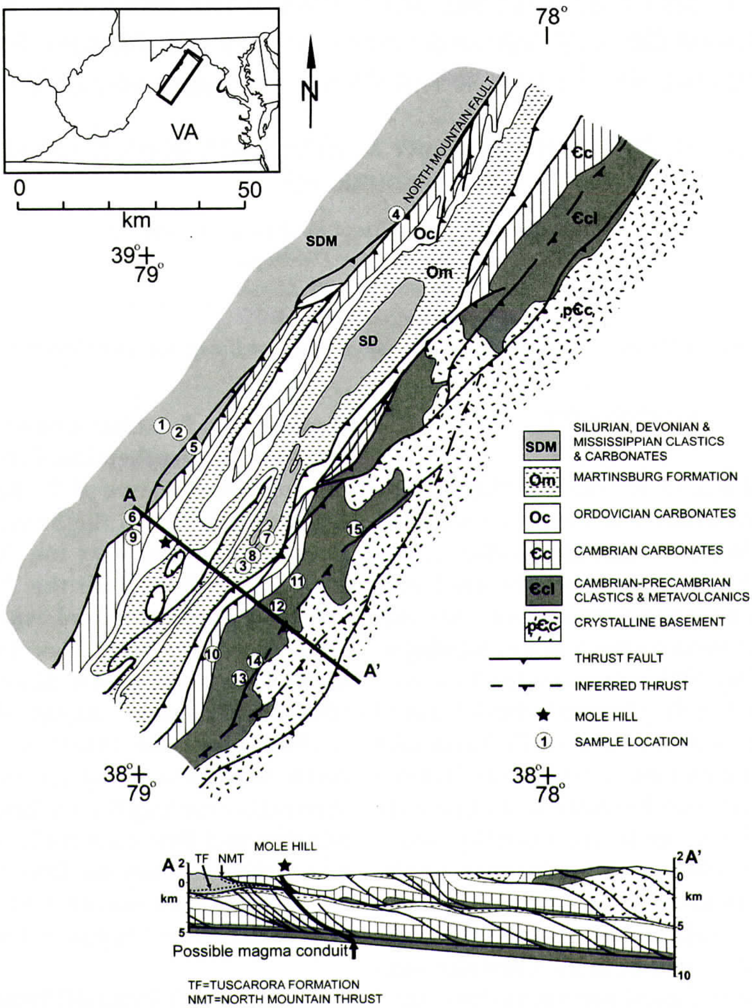

Figure 1. Generalized regional geologic map after Evans (1989). The locations of sandstone units analyzed for this study are labeled with numbers, and the location of Mole Hill is marked with a star. The cross-section based upon seismic reflection data and cross-sections D-D' and E-E' of Evans (1989).

contact zone within the Beekmantown along the north edge of the neck and is interpreted from field and petrographic observations to have formed from hydrothermal silicification of the Beekmantown during emplacement of the basalt (Herbert and Young, 1956).

The Mole Hill basalt is aphanitic to porphyritic, contains microphenocrysts of olivine and clinopyroxene, and has a groundmass of microcrystalline plagioclase, clinopyroxene, olivine, and spinel (Furman and Gittings, 2003; Beard, 2010). Large (up to 2 cm) mantle xenoliths and xenocrysts of clinopyroxene, spinel, olivine, and rare plagioclase (Furman and Gittings, 2003; Beard, 2010; Sacco and Johnson, 2011) occur throughout the volcanic neck. Sandstone xenoliths are concentrated on the southeast slope of the hill. None have been found at the summit, which is interpreted to be the center of the neck. The sandstone xenoliths are approximately 1-50 mm in diameter, are white to tan in hand sample, and are surrounded by reaction rims within the basalt. No xenoliths of Beekmantown or other carbonate rock have yet been found at Mole Hill.

The basalt at Mole Hill is exposed in outcrop as blocky columnar joints 10-20 cm in diameter and 10-40 cm in length. The columnar nature of the basalt is consistent with the interpretation that Mole Hill represents an eroded volcanic neck. Basalt that is now exposed at the surface originally cooled within the conduit. The sandstone and mantle xenoliths are found within these columns, suggesting that the xenoliths were entrained within the basaltic magma during its ascent through the crust and mantle, and were not mixed into the basalt from rock units that originally lay above the present-day erosional surface. This would be a possibility only if the basalt at Mole Hill exhibited a brecciated texture similar to diatremes found elsewhere in the Eocene volcanic field (Tso and Surber, 2006). Therefore, based on field and hand sample observations it is most likely that the sandstone xenoliths originated from rocks below the present-day surface.

In this study, we identify the origin of the sandstone xenoliths at Mole Hill by comparing their textures, including framework grain size and shape and whole-rock geochemistry, to sandstone units exposed within the Shenandoah Valley, Blue Ridge, and folded Appalachians. These data constrain the crustal structure underneath the Shenandoah Valley and provides a mechanism for magma migration through the crust.

Regional Geology

A generalized geologic map and cross-section of the Shenandoah Valley near Mole Hill (Figure 1) based upon seismic reflection data by Evans (1989) shows the spatial distribution of sandstone units in the Shenandoah Valley at the surface and provides an interpretation of where these units may be found within the crust at depth. Sandstones of the Precambrian Swift Run Formation and Cambrian Chilhowee Group (Weverton, Harpers, and Antietam Formations) are exposed along the western flank of the Blue Ridge and in the eastern Shenandoah Valley. The Shenandoah Valley is underlain by Cambrian and Ordovician limestones and dolostones and the Massanutten synclinorium subprovince is comprised of Silurian and Devonian limestones, shales, and sandstones. Silurian, Devonian, and Mississippian strata are found in the western Shenandoah Valley and the folded Appalachians. All of these units were folded and faulted during the Alleghenian Orogeny.

The cross-section in Figure 1 is a compilation of interpretations from the Briery Branch 1:24,000 Quadrangle (Dan Doctor, personal communication) and those presented in cross-section D and cross-section E of Evans (1989) that transect the valley to the north and to the south of Mole Hill, respectively. In the Evans (1989) model, the Shenandoah Valley is underlain by two duplexes. The lower duplex consists of imbricated Cambrian and Ordovician carbonate units above a décollement within the Cambrian and Precambrian clastics and metavolcanics. The upper duplex, or the North Mountain Thrust Sheet, contains a second set of imbricated Cambrian and Ordovician carbonate units with the North Mountain Thrust or an associated fault acting as the décollement. In cross-section E of Evans (1989), the lower duplex is pervaded by smaller thrust sheets separated by numerous splay faults in the western Shenandoah Valley that corresponds to the region underlying Mole Hill. This is the interpretation for the lower duplex shown in cross-section A-A' in Figure 1. The upper duplex is interpreted as a series of fault-bend folds in Evans (1989), with Mole Hill located in the leading edge of the hanging wall of the North Mountain Fault. A cross-section by Southworth and others (1993) transecting the Shenandoah Valley south of Mole Hill shows doubling of the section as in Evans (1989), but has larger, folded thrust sheets of Cambrian and Ordovician units above a décollement within the Cambrian rock units overlain by a second layer of folded Ordovician rocks. Geologic mapping within the Briery Branch 1:24,000 Quadrangle and audio-magnetotelluric (AMT) sounding data indicate the presence of a thrust fault to the west of Mole Hill that is interpreted as a splay of the North Mountain Fault (Pierce and Doctor, 2011). Both Evans (1989) and Southworth and others (1993)

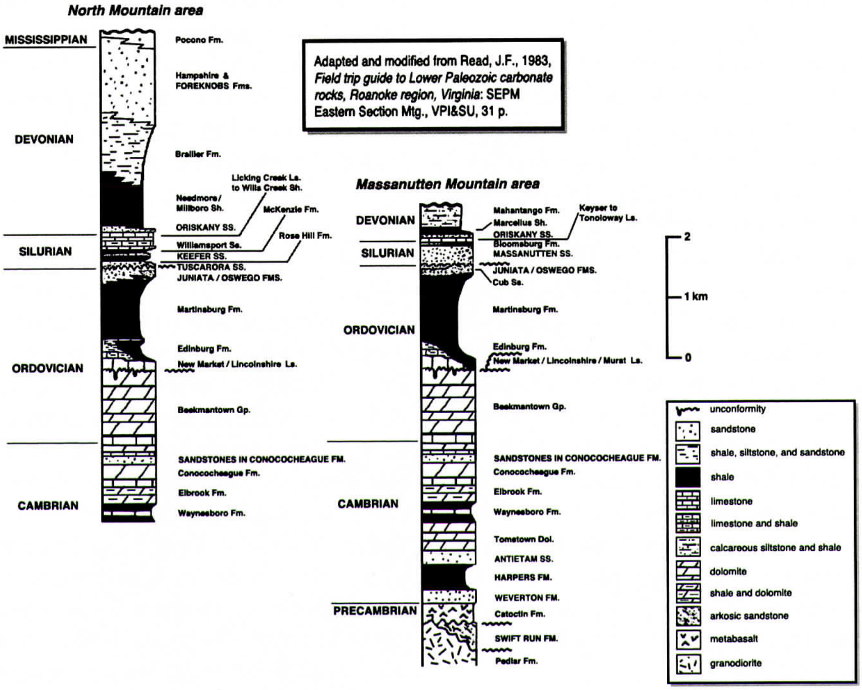

Figure 2. Generalized stratigraphic columns for the Lower and Middle Paleozoic section of west-central Virginia. CAPITALIZED units were sampled for comparison with sandstone xenoliths at Mole Hill. Left column shows the stratigraphy of the several horse blocks west of Mole Hill along the North Mountain structural front, and at exposures in nearby sections west of the North Mountain fault zone. Right column shows the stratigraphy of Massanutten Mountain, east-northeast of Mole Hill.

show the younger Silurian and Devonian units in the footwall of the North Mountain Thrust extending underneath the westernmost part of the Shenandoah Valley in a drag fold. In both sections, the wedge of Silurian rocks, including the Tuscarora Formation, pinch out to the west of Mole Hill. In Figure 1, these younger units are shown as extending farther to the east underneath Mole Hill based on the results from the current study.

Figure 2 is a stratigraphic column (adapted from Read, 1983) containing all of the regional sedimentary formations. Detailed summaries of the characteristics of these formations in the general vicinity of Mole Hill and the central Shenandoah Valley are found in Bartholomew (1977), Gathright and others (1977), Gathright and Frischman (1986), and Rader and Evans (1993). Here, we summarize the petrographic characteristics of the sandstone units relevant to this study. The following abbreviations are used in the descriptions: MRF = metamorphic rock fragment, SRF = sedimentary rock fragment, VRF = volcanic rock fragment, and QFRF = quartzo-feldspathic rock fragment.

The sandstones of the Foreknobs Formation are fine- to medium-grained, lithic to sublithic arenites comprised of subangular to subrounded framework grains of monocrystalline quartz, abundant unstretched polycrystalline quartz and some stretched polycrystalline quartz as well, twinned plagioclase and microcline as well as untwinned orthoclase, some siltstone SRFs and chert grains, and minor to trace amounts of detrital muscovite, zircon, and tourmaline. Quartz overgrowths are common, with dust lines on some of the original detrital grains revealing their true, more rounded shape that is now obscured by the authigenic overgrowths. Sericite and chlorite occur as matrix between a few grains, and these have partially oxidized in some areas to limonite.

The Oriskany Sandstone is a medium-grained, calcite-cemented quartz arenite but silica cements (primarily as optically continuous quartz overgrowths but also as minor pore-reducing chert and chalcedony) are also present in some samples. Monocrystalline quartz is the major framework grain, and some of these grains have a thin coating of limonite. Unlike nearly all of the older sandstones, there are commonly large moldic pore spaces (up to 3cm long) in the Oriskany that formed from dissolution of brachiopod shells and shelly debris as evidenced by the preserved brachiopod shell textures on the walls of many such molds. In thin section, these pores, where present, occur as curved, sweeping voids. A few detrital zircon and tourmaline grains are present.

The Keefer Sandstone is a medium-grained, silica-cemented (by optically continuous quartz overgrowths) quartz arenite. The framework grains are primarily subangular to subrounded monocrystalline quartz, some with thin hematite coatings which impart a pinkish cast to hand samples that is also evident in thin section. A few polycrystalline quartz grains are also present, along with detrital zircon and tourmaline.

The Tuscarora Formation is a medium-grained, silica-cemented (by optically continuous quartz overgrowths) mature to supermature quartz arenite that is >98% subangular to subrounded monocrystalline quartz. The quartz overgrowths commonly meet at 120° angles. Other framework grains include rare polycrystalline quartz and detrital zircon and tourmaline.

Like the facies equivalent Tuscarora and Keefer Sandstones (Roberts and Kite, 1978), the Massanutten Formation is an indurated silica-cemented quartz arenite, but with far more numerous layers of coarse to very coarse to pebbly sand. Being coarser, the Massanutten is immediately recognizable as being texturally less mature than the Tuscarora and Keefer, and it contains more polycrystalline quartz grains along with pebbles and larger sand grains of vein quartz. Nonetheless, the Massanutten sandstone is also compositionally mature, with monocrystalline quartz being the primary framework grain, and optically continuous quartz overgrowths being the principal cement. Detrital zircon and tourmaline occur in trace amounts.

The medium- to coarse-grained sandstones of the Juniata and Oswego Formations are lithic to sublithic arenites comprised of subangular to subrounded framework grains of mostly unstretched polycrystalline quartz with minor stretched polycrystalline, siltstone and mudrock SRFs (some being notably reddish brown in thin section), monocrystalline quartz, some feldspar, a few chert grains, and trace amounts of detrital muscovite, biotite, zircon, and tourmaline. A very few VRFs and QFRFs are present in some Oswego sandstone samples (Rader and Perry, 1976). The Juniata and Oswego sandstone have a sparse sericitic and chloritic matrix (much of which may be derived from squashing of argillaceous SRFs) that in some samples has partially oxidized to limonite and/or hematite, giving hand samples of these formations their characteristic greenish (Oswego) or reddish (Juniata) colors that are also evident in thin section. The Oswego and Juniata Formations are stratigraphically conformable with the Tuscarora Formation, but the Juniata Formation has not been recognized at Cooper Mountain (location 6 in Figure 1), the segment of the North Mountain Fault that is closest to Mole Hill (Rader and Perry, 1976).

The Conococheague Formation contains some thin but laterally persistent beds of medium-grained quartz sandstone in an otherwise carbonate-dominated sequence. These are silica-cemented quartz arenites of primarily subrounded to subangular monocrystalline quartz having both straight and undulose extinction. Dust lines are present in many grains, revealing the rounded shape of the original quartz grain as well as showing equant and optically continuous quartz overgrowths that are a primary cement in these sandstones. Some twinned and untwinned feldspars and unstretched polycrystalline quartz grains are present, along with a few echinoderm fragments with syntaxial overgrowths that contribute to the cementation of the sand. Detrital zircon and tourmaline are rare.

The medium- to very coarse-grained sandstone of the Antietam Formation is a silica-cemented (by optically continuous quartz overgrowths) quartz arenite that has undergone more intense regional deformation than the younger sandstones. Although it is difficult to tell the degree to which the interlocking network of quartz grains seen in thin section is due to quartz overgrowths on detrital quartz grains versus initial deformation of a quartz sandstone into a sub-metamorphic quartzite, there are some obvious quartz overgrowths visible on many quartz grains. Monocrystalline quartz is the primary framework grain, with minor polycrystalline quartz and feldspars. Nearly all of the monocrystalline quartz grains show undulose extinction. Sericite is present as a very thin rind on some grains. Detrital zircon and tourmaline are present in trace amounts.

The fine-grained sublithic sandstone of the Harpers Formation has a moderate to strong metamorphic fabric (granoblastic elongate) from deformation and recrystallization of the phyllosilicate matrix, which is mostly sericite in the samples used in this study, but with minor chlorite and trace biotite also reported (Gathright and others, 1977). Framework grains are principally monocrystalline quartz, nearly all with undulose extinction, and lesser amounts of unstretched and stretched polycrystalline quartz (some of which appear likely to be quartzite MRFs), plagioclase and orthoclase, and some schistose and phyllitic MRFs. There is incipient recrystallization along the grain margins of many quartz grains as well, and because many of the quartz grains are monocrystalline quartz (albeit with undulose extinction), this recrystallization has begun to produce domains of polycrystalline quartz (mostly unstretched) in the samples. The dark color of many of the Harpers sandstones comes from ferroan oxides (magnetite, ilmenite, hematite) in the matrix. Detrital zircon and tourmaline occur in trace amounts.

The sandy to pebbly and moderately ferruginous quartz sandstone of the Weverton Formation has a strong metamorphic fabric. Framework grains are principally monocrystalline quartz, nearly all with undulose extinction, along with variable amounts of unstretched polycrystalline quartz and rare stretched polycrystalline quartz (some of which are likely quartzite MRFs), and some schistose and phyllitic MRFs that are almost certainly derived from erosion of the underlying flood basalts of the Catoctin Formation that have been metamorphosed to greenschist facies (Gathright and others, 1977) and would weather to produce a lithic assemblage that would be a mixture of low-grade metamorphosed VRFs and phyllitic MRFs. The matrix is mostly sericite with some chlorite, epidote, and biotite; on unweathered surfaces this assemblage gives many of the sandstone hand samples a dark greenish color, and on more weathered surfaces the alteration to hematite produces a tan to brown color (Gathright and others, 1977). Stretching and incipient recrystallization of the framework quartz grains has produced small but numerous domains of polycrystalline quartz that are evident in thin section, most noticeably as "tails" of polycrystalline quartz in the stress shadows at the margins of the long axes of the quartz framework grains. Detrital zircon, tourmaline, and magnetite are present in minor to trace amounts.

The poorly sorted immature to submature sandstones of the Swift Run Formation generally have a strong to very strong metamorphic fabric, some with notable foliation, and the unit as a whole has been metamorphosed to greenschist facies (Bartholomew, 1977; Gathright and others, 1977). These metasandstones are medium- to coarse-grained to pebbly, with granules and pebbles of subangular to subrounded vein and polycrystalline quartz being abundant in some beds. The common framework grains are monocrystalline quartz including blue quartz, nearly all with undulose extinction, unstretched and minor stretched polycrystalline quartz some of which is likely quartzite MRFs, moderately to highly altered plagioclase (twinned) and orthoclase (untwinned) feldspar, and QFRFs that are likely derived from weathering and erosion of the underlying granitic and gneissic Grenville basement. Other lithics include phyllitic MRFs. The matrix is a greenschist grade assemblage of mostly sericite, with lesser chlorite, very fine-grained quartz, and epidote. Similar to the Weverton Formation, incipient recrystallization and stretching of the framework grains especially in the stress shadows along the margins of larger grains produced domains of polycrystalline quartz "tails" in the otherwise monocrystalline quartz grains. Detrital zircon, tourmaline, garnet, and magnetite are present in minor to trace amounts.

The contact zone chert is found within the Beekmantown Group. The chert in the contact zone around the Mole Hill basalt is brecciated, vuggy, and silicified. It contains vugs of red and yellow sphalerite (Scherffius, 1969). Several types of breccia and chert are found within the Beekmantown Group (Herbert and Young 1956) in the western Shenandoah Valley. Herbert and Young (1956) classified breccias in the Beekmantown as "sedimentary" or "tectonic" based on textures and mineralogy. Within the tectonic breccia category, "chatter" breccias such as those found at the Bowers-Campbell mine northeast of Mole Hill contain zinc-sulfide mineralization, are spatially associated with igneous rocks, and are interpreted to be hydrothermal deposits. Based on its association with the Mole Hill igneous plug and similar mineralogy and textures, the contact zone chert at Mole Hill is interpreted to be hydrothermal.

METHODS

Samples

Five sandstone xenoliths, ten samples of basalt, and one sample of a hydrothermal chert found within the contact zone between the Mole Hill basalt and the Beekmantown Formation were obtained from Mole Hill (Figure 1). Twenty-three samples from twelve sandstone units were also obtained by collecting in the field or by loan from the Virginia Department of Mines, Minerals, and Energy. Sample locations are shown in Figure 1.

Petrographic Description and Grain Size Measurements

Thin sections of the sandstone xenoliths and of the regional sandstone units were examined under a petrographic microscope for features including framework grain composition, deformation features and other textures within clasts, principal cements, porosity types, and sorting and shape of framework grains. The matrix and grain boundaries in many of the sandstone xenoliths were infiltrated by magma, precluding useful observations of these features.

Grain size distributions were quantified for monocrystalline quartz clasts within four of the sandstone xenoliths, the chert within the Mole Hill contact zone, and four regional sandstones. A poster-sized image of each thin section was created by assembling a mosaic of photographs obtained at 5x magnification using a petrographic microscope. A uniform grid was superimposed on this image. Three hundred clasts were counted for each thin section. The longest and shortest dimension was measured for each monocrystalline quartz clast selected.

Geochemistry

Samples were prepared for whole-rock geochemistry by splitting into chips and removing weathered or altered fragments. Sandstone and basalt samples were ~20-100 g. The sandstone xenolith samples were 3-10 g. Due to the limited size and quantity of the sandstone xenoliths, it was not possible to completely separate perfectly clean sandstone xenolith fragments from areas of the sandstone xenoliths that were infiltrated by the host basalt magma. Major and trace element geochemical analyses of the sandstone units, sandstone xenoliths, and two samples of the basalt were completed by Activation Laboratories Ltd. using ICP and INAA techniques (Hoffman, 1992). Eight additional samples of the Mole Hill basalt were analyzed by ALS Minerals using ICP-AES techniques.

Principal component analysis

A principal component analysis (PCA) was performed using SAS software to summarize the association between 28 major and trace elements within the sandstone xenoliths, excluding P_2O_5, LOI (loss on ignition), S, Sc, and U. PCA is a data-reduction technique that transforms the set of original variables into a new set of linearly uncorrelated variables, which are called principal components (PCs). PCA can be performed on a correlation matrix, **R**, or a covariance matrix, **S**. For the present study, because the magnitudes of the data values (and, hence, the variances) vary largely among the 28 variables, the correlation matrix was used.

PCA begins with a spectral decomposition of the correlation matrix: $\mathbf{R} = \mathbf{E}\boldsymbol{\Lambda}\mathbf{E}'$, where $\boldsymbol{\Lambda}$ is a diagonal matrix containing the eigenvalues, $\lambda_1 \geq \lambda_2 \geq \ldots \geq \lambda_{28}$, and **E** is a square matrix containing the corresponding eigenvectors, $\boldsymbol{e}_1, \boldsymbol{e}_2, \ldots, \boldsymbol{e}_{28}$. The ith PC, $1 \leq i \leq 28$, is calculated by $y_i = \mathbf{Z}\boldsymbol{e}_i$, where **Z** is the data matrix containing the standardized variables, $z_1, z_2, \ldots, z_{28}$.

RESULTS

Textural features of xenoliths

Figure 3 includes representative petrographic images under crossed Nicols for the sandstone xenoliths and regional sandstone units in this study. Our textural comparisons emphasize the fundamental characteristics of the framework grains due to infiltration of basalt along grain boundaries within most of the sandstone xenoliths. In thin section (Figures 3A and B), the sandstone xenoliths of Mole Hill contain predominantly monocrystalline quartz grains with sparse unstretched polycrystalline quartz grains. Most of the monocrystalline quartz grains in the xenoliths exhibit slight to moderate undulatory extinction and contain linear to sublinear or curvilinear tracks of numerous inclusions. These grains exhibit sutured, concavo-convex, and long-edge to long-edge grain contacts; the first two contact types are indicative of pressure solution occurring along grain margins, whereas the third contact type is from the coalescing of quartz overgrowths as cement on individual quartz grains.

Textural features of possible parent sandstones

The contact zone chert (Figure 3C) contains microcrystalline and undeformed quartz as well as larger chalcedony crystals that display a prominent radial crystal habit indicative of crystallization and subsequent growth under dominantly hydrothermal conditions.

The Foreknobs Formation (Figure 3D) contains a few perthitic feldspar grains and stretched polycrystalline quartz grains among the more common monocrystalline quartz grains. Note the highly birefringent sericite between the grains and along veinlets and fractures within two of the grains.

The Oriskany Formation (Figure 3E) consists of monocrystalline quartz grains with few inclusions. The grains exhibit concavo-convex and long-edge to long-edge contacts. Although most show straight extinction, a very few exhibit undulatory extinction. These are most likely multi-cycle grains reworked from one of the Cambrian or Silurian sandstones.

The Keefer Formation (Figure 3F) displays small domains of polycrystalline quartz between some of the larger monocrystalline quartz grains. These could have formed from localized solution transfer along grain boundaries or could be small quartz silt grains that have been cemented by quartz overgrowths. Sericite is visible along some grain boundaries.

The Tuscarora Formation (Figures 3G, 3H) also consists predominantly of monocrystalline quartz grains, several of which show well-developed quartz overgrowths that meet at 120°, a characteristic texture of silica-cemented sandstones that results from the intersection of crystal faces on three adjoining overgrowths. These grains also exhibit concavo-convex and long-edge to long-edge contacts and contain numerous linear, sublinear, and curvilinear inclusion tracks. In Figure 3H, a narrow domain of polycrystalline quartz is present along the contact between monocrystalline quartz grains.

The sample of the Massanutten Formation shown in Figure 3I consists of monocrystalline quartz grains with concavo-convex and long-edge to long-edge contacts, and most of these

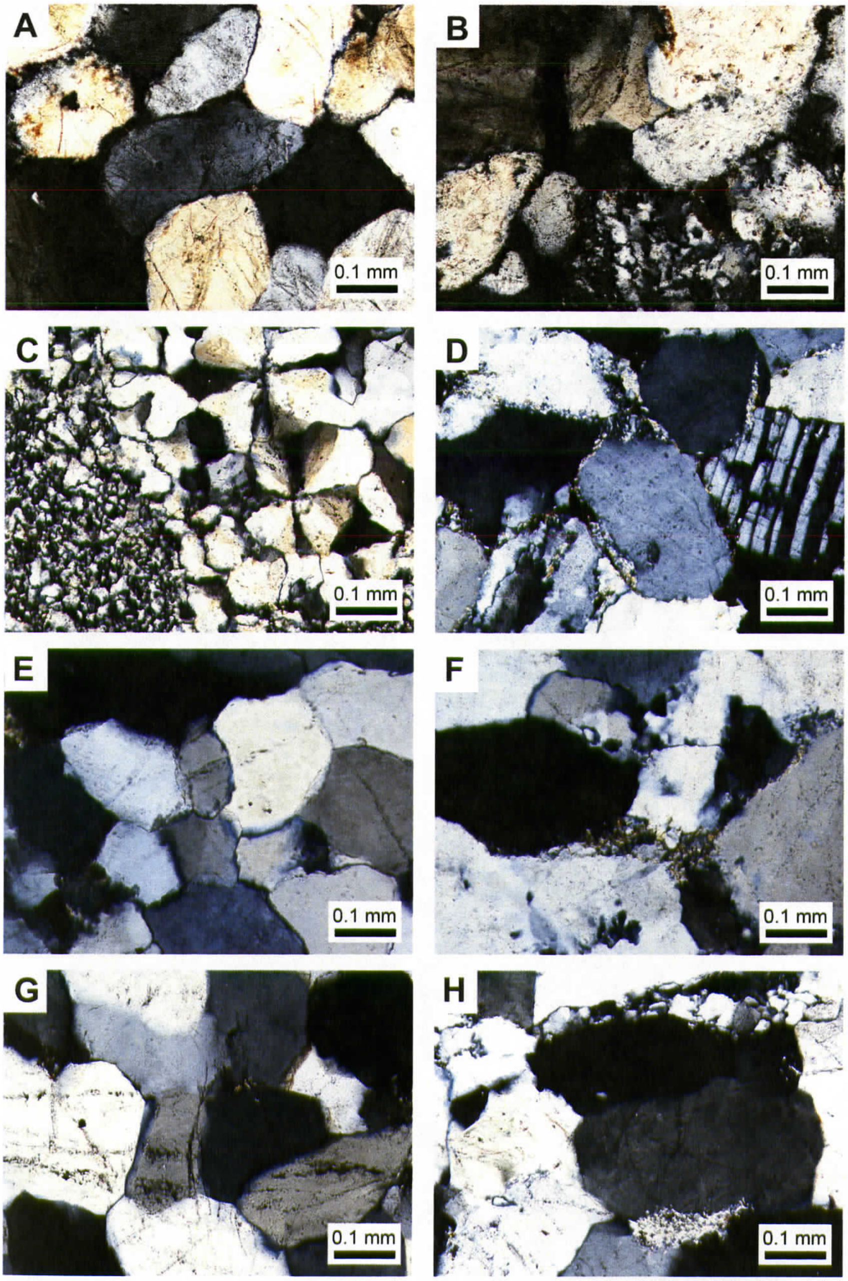

Figure 3. Representative petrographic thin section images of the Mole Hill sandstone xenoliths and the sandstone and quartzite units from the region. Images were obtained under crossed Nichols at 20x magnification and are presented in stratigraphic order, from youngest to oldest. Sample numbers are listed in parentheses. A. Mole Hill sandstone xenolith (0.12); B. Mole Hill sandstone xenolith (1.14); C. Hydrothermal chert breccia in Beekmantown Formation within the contact zone around the Mole Hill basalt (AW1.01); D. Foreknobs Formation (11LJLDRChem); E. Oriskany Formation (11LJFulksDriB); F. Keefer Formation (11LJNMKeefer); G., H. Tuscarora Formation (Tuscarora2ZK);

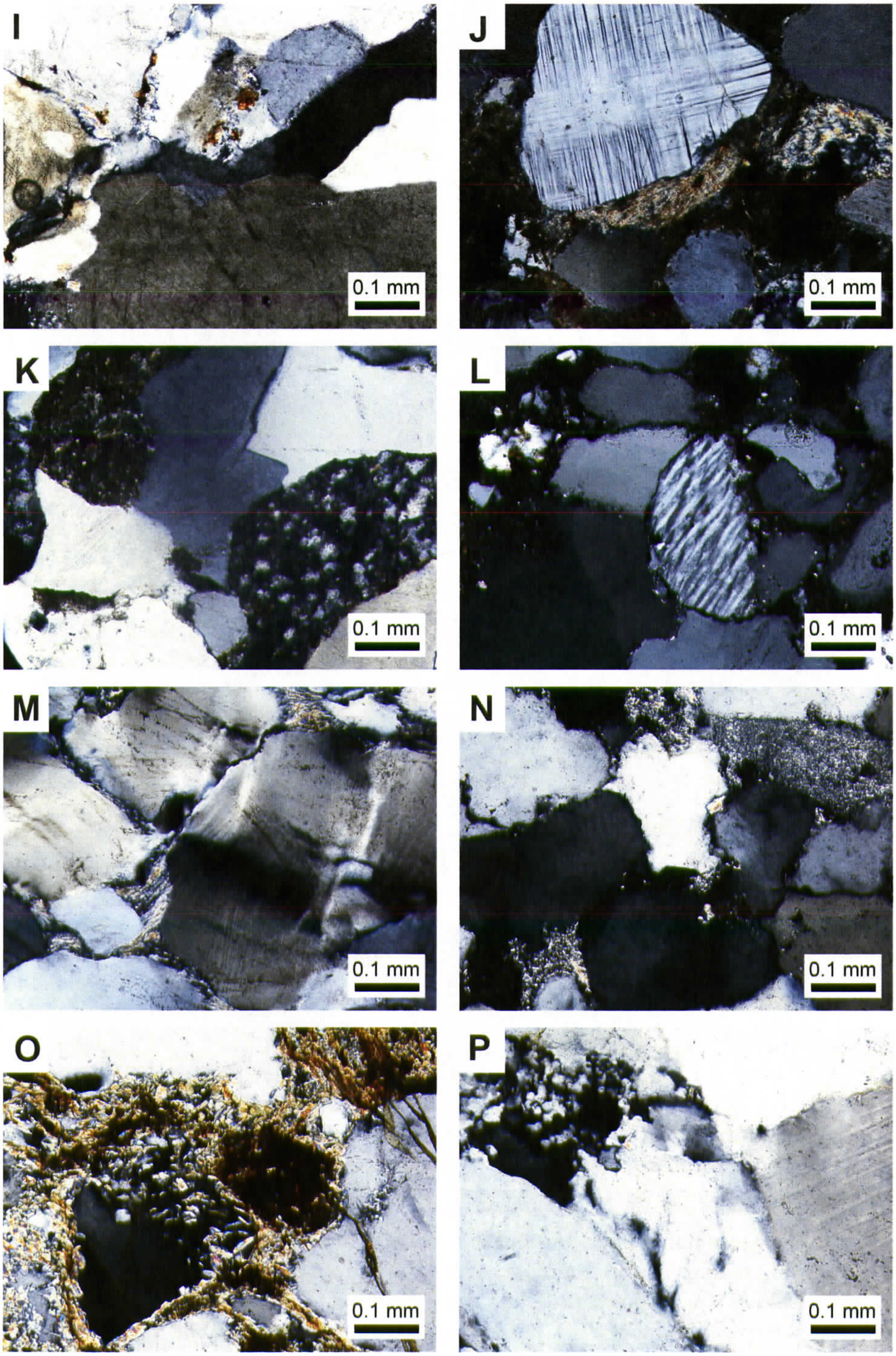

Figure 3. Continued — I. Massanutten Formation (R-10114); J. Juniata Formation (11LJBrocksJun); K. Oswego Formation (11LJBrocksSr2); L. Conococheague Formation (Conococheague ZK); M. Antietam Formation (LJAnt1Elkton); N. Harpers Formation (Harpers); O. Weverton Formation (Weverton) P. Swift Run Formation (Swift Run 1).

grains contain numerous linear to sublinear to curvilinear inclusion tracks. Small and discontinuous patches of hematite (reddish brown areas) and sericite are present along the rims of some quartz grains.

The Juniata Formation (Figure 3J) includes a prominent microcline grain among several monocrystalline quartz grains including one with slight undulatory extinction, and a polycrystalline quartz grain. This sample is notable for its prominent sericitic matrix, the brown color of which may result from a minor amount of organic material or from oxidized iron disseminated throughout the clay.

The Oswego Formation (Figure 3K) includes two siltstone SRFs and a mudrock SRF. These are set among several monocrystalline quartz grains including some with distinct angular contacts that result from the junction of optically continuous quartz overgrowths on the framework quartz grains. The two largest SRFs in the field of view differ in their size and color, with the finer grained SRF at upper left being a more sericite- and probably iron-rich grain (as indicated by its patchy reddish brown color), versus the siltstone SRF at lower right with its numerous quartz silt grains and lesser matrix.

The Conococheague Formation (Figure 3L) includes a perthitic feldspar among several medium-grained monocrystalline quartz grains as well as some quartz silt grains scattered about between the larger quartz sand grains. A matrix of principally sericite occurs discontinuously between some of the larger framework quartz grains as well as between the numerous quartz silt grains.

The sample of the Antietam Formation (Figure 3M) includes a large monocrystalline quartz grain with pronounced undulatory extinction and Boehm lamellae; both features indicate that the grain has been deformed and compressed or torqued to some extent. There are linear to curvilinear inclusion tracks in this and several of the other quartz grains in the field of view. A sericite matrix of varying thickness is present between most of the quartz grains, and in two areas adjacent to the largest quartz grain this matrix exhibits a notable preferred orientation of the phyllosilicate layers, evident from the curvilinear and subparallel fabric of these two domains of the matrix. It is also possible that these two areas of matrix are in fact phyllosilicate-rich SRFs that have been squeezed and deformed during compaction by the many adjacent quartz grains.

The Harpers Formation (Figure 3N) includes a prominent lithic fragment at upper right that is either a chert grain or a silicified shale SRF, which is set among several monocrystalline quartz grains a few of which show long-edge contacts indicative of quartz overgrowths that have coalesced. These quartz grains also lack any obvious inclusion tracks. Two patches of predominantly sericite are very likely deformed mudrock SRFs that were squeezed between the much harder quartz grains, and the deformation of these lithic grains has produced a pseudomatrix in these areas. These areas are identified as patches of pseudo-matrix produced from deformation of phyllosilicate-rich SRFs rather than as true matrix because of the overall lack of a matrix between the other framework grains.

The sample of the Weverton Formation (Figure 3O) contains an abundant sericitic matrix surrounding monocrystalline quartz grains that lack inclusion tracks.

The Swift Run Formation (Figure 3P) shows the contact of a polycrystalline quartz grain with a few monocrystalline quartz grains, two of which are adjacent to a plagioclase grain. Note the lack of appreciable matrix between the grains, and the lack of inclusion tracks in the quartz grains.

Clast size and shape

Histograms of long-axis and long axis/short axis measurements of monocrystalline quartz grains from one representative sandstone xenolith and five of the sandstone units are shown in Figure 4. The long axis to short axis ratio is an indicator of the degree of sphericity of framework grains within each rock.

Quartz grain size and shape were determined for four separate sandstone xenoliths. The average long axis of monocrystalline quartz grains for the xenoliths (n=4) is 0.32 ± 0.12 mm. The average long axis to short axis ratio is 1.98. Of

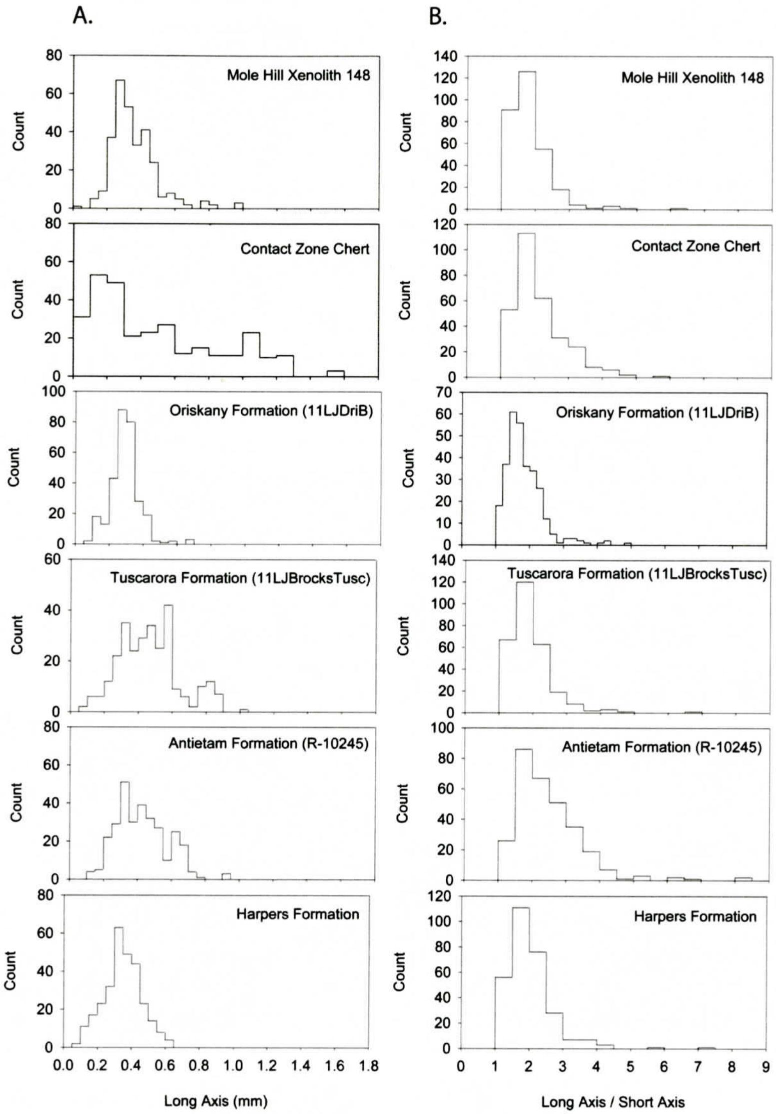

Figure 4. Histograms of A. longest axis (mm) and B. longest axis / shortest axis measurements of monocrystalline quartz clasts in a representative Mole Hill xenolith (148) and five sandstone units.

the measured regional sandstones, many had grain size distributions and long axis to short axis ratios that are similar to those of the sandstone xenoliths, with two exceptions. The contact zone chert has a larger range of grain sizes (0-1.5 mm) including a significant number of very small (<0.1 mm) quartz grains. The Antietam Formation has a significant population of grains with long to short axis ratios > 3, in contrast to the xenolith grains, almost all of which have long to short axis ratios <3.

Geochemistry

Whole-rock geochemical data for the sandstone xenoliths, Mole Hill basalt, and regional sandstone formations are listed in Table 1. The results of the PCA show that the first few PCs

Table 1. Whole-rock geochemical analyses of the Mole Hill basalt, sandstone xenoliths within the Mole Hill basalt, and sandstone units in the Shenandoah Valley and Allegheny Plateau.

Formation:	Sandstone Xenoliths				
Age:	Unknown				
Sample Number	145	147	148	XENO 8	XENO 7
Location	Mole Hill	Mole Hill	Mole Hill	Mole Hill	Mole Hill
Analysis Source	ACT	ACT	ACT	ACT	ACT
SiO_2	90.26	90.1	94.4	94.33	89.22
Al_2O_3	2.41	2.69	1.2	0.72	2.8
$Fe_2O_{3\,T}$	2.09	2.08	1.29	1.94	2.9
MnO	0.04	0.06	0.54	0.04	0.19
MgO	1.1	0.38	0.25	0.58	0.93
CaO	0.56	0.36	0.32	0.14	0.44
Na_2O	0.23	0.16	0.09	0.12	0.18
K_2O	0.6	0.44	0.3	0.15	0.91
TiO_2	0.253	0.277	0.149	0.044	0.434
P_2O_5	0.02	0.03	0.16	< 0.01	0.05
LOI	3.32	2.73	1.73	1.09	2.5
Total	100.9	99.31	100.4	99.16	100.6
Ba	504	597	1420	46	385
Co	5	6	11	6	22
Cr	10	10	13	11	19
Cu	21	100	191	164	178
Hf	2.1	3	2.9	1	6.6
Ni	9	14	21	18	38
S (%)	0.003	0.017	0.024	0.018	0.003
Sc	2.9	2.9	1.8	0.8	4
Sr	54	33	29	9	48
Th	2.9	2.7	1.4	< 0.5	2.9
U	< 0.5	< 0.5	< 0.5	< 0.5	< 0.5
V	17	15	14	< 5	29
Y	12	7	7	7	9
Zn	15	35	30	9	24
Zr	57	91	68	28	212
La	12.8	14.7	9.9	8.6	13.9
Ce	18	11	16	13	24
Nd	< 5	< 5	10	13	< 5
Sm	1.8	1.6	1.3	2.6	2.4
Eu	0.5	< 0.1	0.3	0.5	0.6
Yb	1.4	1.1	1	0.3	1.4
Lu	0.3	0.18	0.14	0.1	0.24

Formation:	Mole Hill Basalt									
Age:	Eocene									
Sample Number	1.11	1.12	1.13	1.15	1.16	1.18	1.19	1.2	Xeno8	1.03
Location	Mole Hill	Mole Hill	Mole Hill	Mole Hill	Mole Hill	Mole Hill	Mole Hill	Mole Hill	Mole Hill	Mole Hill
Analysis Source	ALS	ALS	ALS	ALS	ALS	ALS	ALS	ALS	ACT	ACT
SiO_2	44.2	44.8	45.6	44.5	45.1	44.3	44.5	45	46.53	46.08
Al_2O_3	14.5	14.8	14.9	14.85	15.05	14.45	15.1	15.15	15.14	15.28
$Fe_2O_{3\,T}$	12.45	12.05	12.45	12.55	12.55	11.9	12.4	12.3	11.8	11.95
MnO	0.2	0.2	0.21	0.21	0.21	0.21	0.21	0.21	0.2	0.2
MgO	9.69	9.41	9.32	8.93	8.82	9.46	9.28	9.34	9.2	9.86
CaO	11.75	12.25	12.1	11.1	11.35	11.8	11.55	11.55	11.38	11.6
Na_2O	2.13	2.18	2.12	2.24	2.18	2.12	2.2	2.15	2.27	2.29
K_2O	0.73	0.7	0.8	0.75	0.81	0.83	0.84	0.82	0.8	0.72
TiO_2	1.55	1.57	1.6	1.57	1.61	1.55	1.59	1.62	1.615	1.641
P_2O_5	0.34	0.36	0.37	0.37	0.38	0.37	0.34	0.38	0.37	0.37
LOI	0.6	1.39	0.7	1.3	1.56	1.65	0.1	0.4	0.9	0.65
Total	98.3	99.9	100.5	98.5	99.8	98.8	98.3	99.1	100.2	100.9
Ba	426	417	441	467	481	463	460	478	441	440
Co	56	54.1	55.4	52	50.5	53.5	52.4	52.3	57	57
Cr	310	390	340	310	280	390	320	340	285	305
Cu	68	75	72	75	80	75	72	84	65	63
Hf	3	3	2.9	2.4	2.6	2.4	2.4	2.5	2.9	2.8
Ni	177	164	181	198	183	205	199	205	179	174
S (%)	nd	nd	nd	nd	nd	nd	nd	nd	0.013	0.011
Sc	nd	nd	nd	nd	nd	nd	nd	nd	34.6	36.4
Sr	551	526	654	549	653	593	592	662	579	523
Th	4.01	3.78	4.07	3.94	3.88	3.8	3.82	3.89	4.9	4.1
U	1.09	1.09	1.04	0.92	0.94	0.85	0.86	0.89	1.2	<.5
V	252	254	257	272	254	274	270	265	263	272
Y	26.9	26.3	28.9	31.1	31.2	30.4	30.8	31	29	28
Zn	88	87	89	88	94	91	92	91	63	59
Zr	110	103	108	104	106	101	100	103	101	97
La	30.4	29.1	30.1	30.8	31.2	30.1	30.5	31.1	33	32.9
Ce	50.3	48.7	50.3	56.2	57.8	55.5	56.3	56.5	57	55
Nd	24.6	23.4	24.5	24.9	25.2	24.4	24.5	24.1	28	25
Sm	5.24	4.81	5.05	4.91	5.21	4.97	4.97	4.99	4.1	4
Eu	1.92	1.76	2	1.7	1.7	1.71	1.74	1.72	2	1.9
Yb	3.14	3.03	3.68	3.44	3.43	3.17	3.32	3.5	3.3	3.5
Lu	0.51	0.44	0.57	0.51	0.54	0.48	0.51	0.53	0.54	0.56

Formation:	Hydrothermal Chert	Foreknobs	Oriskany		Keefer
Age:	Eocene	Devonian	Devonian		Silurian
Sample Number	AW 1.01	11LJLDRChem	11LJFulksDriA	R-10113	11LJNMKeefer
Location	Mole Hill	1	2	3	4
Analysis Source	ACT	ACT	ACT	ACT	ACT
SiO_2	98.55	96.19	98.11	94.62	94.3
Al_2O_3	0.52	1.47	1.17	2.37	2.99
$Fe_2O_{3\,T}$	1.03	2.08	0.86	1.63	0.71
MnO	0.13	0.02	0.01	< 0.01	< 0.01
MgO	0.05	0.06	0.06	0.24	0.14
CaO	0.08	0.02	0.03	0.16	0.04
Na_2O	0.02	0.19	0.02	0.03	0.03
K_2O	0.05	0.21	0.19	0.35	0.88
TiO_2	0.035	0.08	0.07	0.176	0.219
P_2O_5	< 0.01	0.01	0.02	0.09	< 0.01
LOI	0.22	0.29	0.29	0.74	0.37
Total	100.7	100.6	100.8	100.4	99.7
Ba	75	29	131	43	46
Co	22	2	3	5	5
Cr	13	6	8	11	8
Cu	4	4	3	4	3
Hf	< 0.5	2.2	4.5	4.5	4.3
Ni	14	6	7	9	5
S (%)	0.035	0.003	0.003	0.238	0.004
Sc	1.1	0.8	0.6	2.1	1.9
Sr	6	8	18	7	10
Th	< 0.5	1	1.1	2.1	4
U	< 0.5	< 0.5	< 0.5	1.4	1
V	13	6	< 5	10	9
Y	< 1	4	9	10	10
Zn	13	12	9	6	4
Zr	12	76	171	180	138
La	1.3	4.8	8.6	9.3	14.7
Ce	11	11	16	18	29
Nd	< 5	< 5	< 5	<5	10
Sm	< 0.1	1.1	2.1	2.5	1.9
Eu	< 0.1	0.3	0.5	0.6	0.5
Yb	< 0.1	0.6	0.8	1	1.4
Lu	< 0.05	0.1	0.13	0.25	0.22

Formation	Tuscarora				Massanutten		
Age:	Silurian				Silurian		
Sample Number	11LJFulks Clinch	11LJBrocksT usc	Tuscarora 1ZK	Tuscarora 2ZK	R-10109	R-10114	R-10115
Location	2	5	6	6	7	8	8
Analysis Source	ACT	ACT	ACT	ACT	ACT/ DMME	ACT/ DMME	ACT/ DMME
SiO_2	94.8	99.2	96.2	97.6	98.47	95.94	97.49
Al_2O_3	0.87	0.28	1.8	0.42	1.01	1.09	0.7
$Fe_2O_{3\,T}$	2.07	0.55	1.41	0.92	0.58	0.46	0.44
MnO	0.01	<.01	0.01	<.01	0.004	0.002	0.002
MgO	0.02	<.01	0.15	0.02	0.04	0.02	<.01
CaO	0.01	<.01	0.03	0.02	0.02	0.02	0.01
Na_2O	0.02	0.01	0.03	0.04	0.08	0.08	0.08
K_2O	0.18	0.08	0.82	0.11	0.3	0.2	0.1
TiO_2	0.077	0.047	0.067	0.043	0.143	0.11	0.054
P_2O_5	0.02	<.01	0.01	<.01	0.02	0.02	0.03
LOI	0.2	-0.1	0.28	0.15	0.31	0.55	0.31
Total	98.28	100.1	100.8	99.32	101	98.49	99.22
Ba	41	14	75	12	71	18	21
Co	<1	<1	2	2	3.4	<.1	1.1
Cr	8	6	12	8	85.8	103	64.8
Cu	6	10	5	5	8	4	9
Hf	3	2.1	1.3	1.8	8.4	5.2	2.2
Ni	3	2	6	4	3	3	4
S (%)	0.019	0.003	0.003	0.004	0.004	0.003	0.003
Sc	1	0.5	1	0.5	0.89	0.97	0.54
Sr	7	4	6	5	4	4	4
Th	1.8	<.5	2.6	0.9	6.2	5.9	2.3
U	<.5	<.5	0.5	<.5	1.9	1.3	0.5
V	6	<5	6	<5	6	8	<5
Y	3	3	6	2	9	8	4
Zn	28	<1	5	2	3	3	3
Zr	106	78	51	67	301	139	67
La	11.4	8	8.2	3.7	13.4	11.5	7.93
Ce	27	24	16	8	26	23	18
Nd	13	22	<5	5	12	9	7
Sm	2.1	4.6	0.8	0.5	2.24	1.58	1.02
Eu	0.3	0.8	0.3	0.2	0.36	0.27	0.18
Yb	0.6	0.3	0.5	0.4	1.4	1.14	0.51
Lu	0.11	0.1	0.09	0.05	0.23	0.16	0.08

Formation:	Juniata	Oswego		Conococheague	
Age:	Ordovician	Ordovician		Cambrian	
Sample Number	11LJBrocksJun	11LJBrocksOos	11LJBrocksSr2	ConococheagueZK	R-10096
Location	5	5	5	9	10
Analysis Source	ACT	ACT	ACT	ACT	ACT
SiO_2	80.23	82.19	83.47	97.62	82.92
Al_2O_3	6.92	8.7	6.61	0.94	0.39
Fe_2O_{3T}	5.81	3.05	4.72	1.07	0.71
MnO	0.03	0.02	0.05	<.01	0.01
MgO	1.43	1.21	1.32	0.03	3.2
CaO	0.23	0.06	0.35	0.04	5.64
Na_2O	0.04	0.48	0.1	0.01	0.02
K_2O	2.38	3.07	1.8	0.67	0.23
TiO_2	0.952	0.44	0.498	0.022	0.017
P_2O_5	0.09	0.02	0.11	0.02	0.01
LOI	1.71	1.7	1.68	0.07	7.75
Total	99 81	100.9	100.7	100.5	100.9
Ba	229	275	214	45	23
Co	10	8	10	2	<1
Cr	37	35	43	9	6
Cu	9	6	14	4	3
Hf	5.6	7	6.6	1.9	1.1
Ni	21	14	24	4	1
S (%)	0.006	0.01	0.1	0.003	0.008
Sc	9.4	5.6	7.4	0.8	1
Sr	22	32	37	4	26
Th	4.2	5.6	5.6	0.6	<.5
U	1.6	1.6	1.6	<.5	<.5
V	120	35	54	7	<5
Y	17	14	18	<1	3
Zn	35	34	41	2	4
Zr	181	212	218	68	33
La	22.4	26.7	32.8	1.2	3.2
Ce	45	48	62	<3	<3
Nd	22	14	22	<5	<5
Sm	4	2.9	5.1	0.2	0.5
Eu	1.1	0.8	1.3	<.1	0.3
Yb	2.7	2.2	2.2	0.2	0.5
Lu	0.34	0.35	0.3	<.05	<.05

Formation:	Antietam				Harpers	Weverton	Swift Run
Age:	Cambrian				Cambrian	Cambrian	Precambrian
Sample Number	LJAnt1Elkton	LJAnt2Elkton	104	Elkton/340	Harpers	Weverton	Swift Run 1
Location	11	11	12	11	13	14	15
Analysis Source	ACT	ACT	ACT	ACT	ACT	ACT	ACT
SiO_2	93.9	97.55	95.21	97.81	98.47	82.87	91.52
Al_2O_3	2.57	1.44	1.96	1.51	0.94	6.13	4.34
$Fe_2O_{3\,T}$	0.76	0.83	0.62	0.76	0.79	5.49	0.94
MnO	< 0.01	0.02	< 0.01	< 0.01	< 0.01	0.01	0.02
MgO	0.15	0.08	0.03	0.05	0.03	0.55	0.11
CaO	< 0.01	0.01	< 0.01	0.02	0.01	0.02	0.82
Na_2O	0.01	< 0.01	< 0.01	< 0.01	0.01	0.02	0.04
K_2O	0.59	0.35	0.08	0.17	0.17	2.26	0.76
TiO_2	0.312	0.176	0.249	0.152	0.247	1.225	0.13
P_2O_5	0.01	0.02	0.02	0.03	0.02	0.13	0.01
LOI	0.38	0.32	0.41	0.17	-0.05	1.46	0.87
Total	98.7	100.8	98.6	100.7	100.6	100.2	99.56
Ba	51	89	27	82	166	359	168
Co	2	2	2	2	<1	3	3
Cr	11	8	11	8	8	21	10
Cu	4	7	2	5	2	3	40
Hf	13	7.8	10.9	5.9	5.3	17.1	5.8
Ni	7	4	1	5	4	7	8
S (%)	< 0.001	0.003	<.001	<.001	0.002	<.001	0.002
Sc	2.4	1.9	1.1	1.1	1.5	8.7	1.3
Sr	< 2	3	6	6	29	7	156
Th	2.1	1.9	2.1	1.4	1	6.6	2.1
U	1	< 0.5	1	<.5	<.5	<.5	<.5
V	21	14	8	8	6	73	6
Y	10	11	5	7	12	9	4
Zn	3	5	2	2	1	19	6
Zr	484	258	396	189	171	657	222
La	14.6	11.5	20.6	7.8	14.3	32	8.5
Ce	27	24	43	19	32	66	13
Nd	< 5	< 5	14	10	12	36	<5
Sm	1.4	1.9	2.2	1.8	2.7	5.4	1
Eu	0.5	0.5	0.5	0.5	0.8	1.2	0.5
Yb	1.9	1.8	1.3	1	1.5	1.4	0.8
Lu	0.29	0.34	0.19	0.19	0.22	0.27	0.13

account for a large portion of the variability in the data. The eigenvalues of the first five PCs are$\lambda_1 = 19.96$, $\lambda_2 = 3.70$, $\lambda_3 = 1.65$, $\lambda_4 = 0.78$, and $\lambda_5 = 0.55$. Careful examination of the eigenvectors (see Table 2) reveals that the first three PCs, which account for a total of 90.4% of the data variability, lend themselves to meaningful interpretations.

PC1 accounts for 71.3% of the variability in the data. This PC gives heavy positive weights to Al_2O_3, Fe_2O_{3T}, MgO, and Ni and a heavy negative weight to SiO_2. Therefore, PC1 is interpreted as a measure of the influence of infiltration of the basaltic magma into the sandstone xenoliths. PC2 accounts for 13.2% of the data variability. PC2 includes Hf, Zr, and K_2O as important components, and it is interpreted as a measure of the contributions of trace minerals including zircon and clays to the compositions of the original sandstone formations. PC3 accounts for only 5.9% of the data variability. PC3 gives heavy weights to Ba, MnO, and other elements that are mobilized during hydrothermal or hydrous alteration. Therefore, the elements in PC1 represent those that are representative of contamination of the sandstone xenoliths by the basaltic magma and can be used to leverage the original sandstone composition from the sandstone xenoliths.

Figure 5 shows a plot of PC2 versus PC1. The basalt data fall in a tight cluster at positive values of PC1 and around 0 for PC2. The quartz-bearing sandstone xenoliths contain high SiO_2 as well as variable amounts of clays and zircon (Hf, Zr, and K_2O-bearing minerals). They are found in a region that has a narrow range of negative PC1 values and a wide range of PC2 values. The regional sandstone formations tend to have more negative PC1 values and similar or more positive PC2 values compared to the xenoliths. A mixing trend can be extended between the basalt and sandstone xenoliths. The sandstone unit from which the xenoliths originated should plot to the left of the xenoliths along this trend. The sandstone units that fall within the possible end-member space are from the Tuscarora, Foreknobs, and Conococheague Formations. The contact zone chert also falls within this end-member space. The Oriskany and Massanutten Formations each have one data point within this end-member region.

DISCUSSION

Table 3 summarizes the lines of evidence supporting or rejecting each sandstone unit as the parent body of the sandstone xenoliths at Mole Hill. The combined criteria support the Silurian Tuscarora Formation as the most likely source of sandstone xenoliths at Mole Hill.

Some sandstone units have a characteristic color or texture in hand sample that is significantly different from the appearance of the sandstone xenoliths in thin section. The hydrothermal chert in the contact zone at Mole Hill contains numerous vugs filled with euhedral quartz crystals and fine-grained oxides. The Foreknobs Formation is a brown-grey color, too dark to match the appearance of the xenoliths. The Oswego and Juniata Formations are cross-bedded dark gray to dark red sandstones in hand sample, and being lithic arenites they are completely different compositionally from the sandstone xenoliths, which are quartz arenites. The Conococheague sandstones that were collected close to Mole Hill are medium gray on fresh surfaces and are calcareous, with notable thin laminae that consist primarily of calcite. The Harpers, Weverton, and Swift Run Formations are lithic to subarkosic and poorly-sorted sandstones, and have overall larger clast sizes than the xenoliths. Additionally, these Lower Cambrian sandstones exhibit a pervasive weak to prominent metamorphic fabric including polycrystalline quartz "tails" in the stress shadows of many of the quartz grains, a distinctive fabric that is not seen in any of the xenoliths. The best matches to the sandstone xenoliths in hand sample are the most quartz-rich sandstones, which are tan to white in hand sample; these include the quartz arenites of the Oriskany, Keefer, Tuscarora, Massanutten, and Antietam Formations. No fossil fragments or biomoldic pores were observed in any of the sandstone xenoliths.

Thin sections of the Tuscarora and Oriskany

Table 2. Eigenvectors for the First Three Principal Components

Elem	e_1	Elem	e_2	Elem	e_3
Fe_2O_3	.221	Hf	.461	Ba	.593
V	.221	Zr	.454	Cu	.535
Al_2O_3	.221	K_2O	.335	MnO	.459
TiO_2	.220	Th	.321	Hf	.154
Y	.218	Ce	.248	K_2O	.147
Ni	.216	La	.201	Zr	.117
Na_2O	.216	Nd	.169	Th	.070
MgO	.215	Sm	.165	SiO_2	.065
Zn	.215	Lu	.095	La	.048
Eu	.215	Yb	.087	Zn	.033
Sr	.214	Eu	.068	Ce	.005
Co	.214	SiO_2	.049	Lu	-.003
Cr	.212	TiO_2	.048	Sm	-.003
Yb	.211	Al_2O_3	.016	Nd	-.004
CaO	.210	Y	.015	Yb	-.010
Lu	.208	Fe_2O_3	-.030	TiO_2	-.021
La	.202	V	-.041	Co	-.028
Sm	.189	Zn	-.068	Y	-.039
Ce	.189	Cr	-.084	Fe_2O_3	-.051
Nd	.178	MgO	-.100	Al_2O_3	-.053
MnO	.146	Na_2O	-.101	Ni	-.064
Th	.123	Ba	-.103	Eu	-.071
Ba	.119	Ni	-.106	V	-.074
Cu	.094	Sr	-.107	Sr	-.091
K_2O	.073	Co	-.115	Na_2O	-.093
Zr	-.020	CaO	-.126	MgO	-.105
Hf	-.029	MnO	-.203	Cr	-.116
SiO_2	-.220	Cu	-.212	CaO	-.124

Formations show that these units characteristically have framework grain assemblages and textures that are closest to those of the sandstone xenoliths. The sandstones of both the Tuscarora and Oriskany consist of predominantly monocrystalline quartz grains, some of which exhibit slightly undulatory extinction, and nearly all of which have concavo-convex and long-edge to long-edge grain contacts. The monocrystalline quartz grains in the Tuscarora contain linear to curvilinear inclusion tracks that are very similar to those observed in quartz framework grains within the sandstone xenoliths. The monocrystalline quartz grains in the Tuscarora Formation are also pervasively cemented by optically continuous quartz overgrowths that are very similar in texture and fabric to those in the sandstone xenoliths. The quartz grains in the Oriskany thin section lack both the abundant inclusion tracks and the ubiquitous quartz overgrowths of the sandstone xenoliths.

The shape and size of monocrystalline quartz grains are important textural parameters that can be affected by sediment source(s), transport mechanism(s) and distance from source to sink, the final depositional environment and subsequent diagenetic environments during shallow burial and lithification, and then by deformation and elongation processes that affect the sediments during deeper burial, deformation, and incipient metamorphism. The sandstone units

Table 3. Summary of sandstone characteristics consistent with (=Y), possibly consistent with (=Y?), or not consistent with (=N) the characteristics of the Mole Hill sandstone xenoliths. NM = not measured on this sample

Age	Unit	Hand Sample Characteristics	Clast Characteristics in Thin Section	Clast Size and Shape	Geochemical Analyses	Structural Mechanism
EOCENE	Hydrothermal Chert in Contact Zone	N	N	N	Y	Y
DEVONIAN	Foreknobs Fm.	N	N	NM	Y	N
	Oriskany Fm.	Y	Y?	Y	Y?	Y
SILURIAN	Keefer Fm.	Y	N	NM	N	Y
	Tuscarora Fm.	Y	Y	Y	Y	Y
	Massanutten Fm.	Y	N	NM	Y?	N
ORDOVICIAN	Juniata Fm.	N	N	NM	N	Y
	Oswego Fm.	N	N	NM	N	Y
CAMBRIAN	Conococheague Fm.	N	N	NM	Y	Y
	Antietam Fm.	Y	N	N	N	N
	Harpers Fm.	N	N	Y	N	N
	Weverton Fm.	N	N	NM	N	N
PRECAMBRIAN	Swift Run Fm.	N	N	NM	N	N

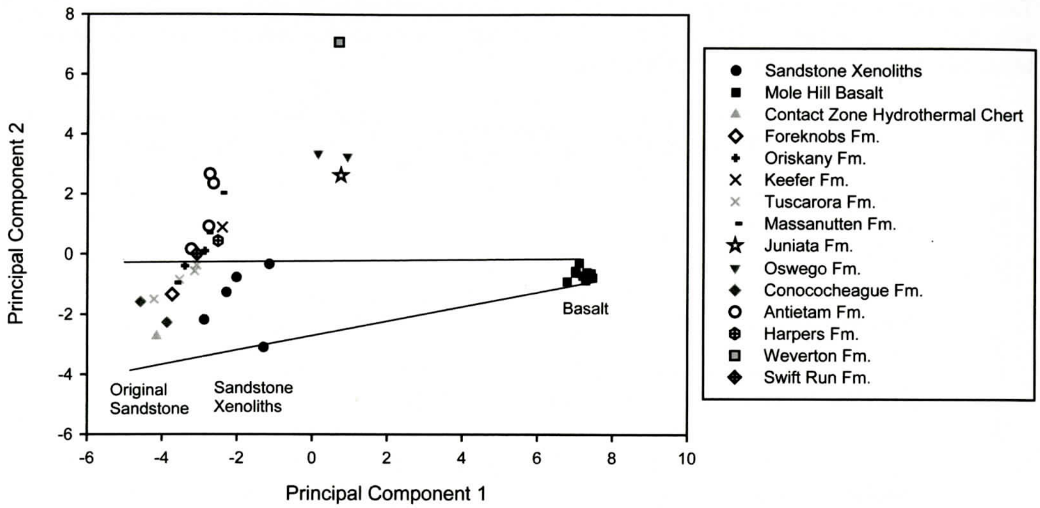

Figure 5. Geochemical data for the Mole Hill basalt, sandstone xenoliths, and regional sandstones plotted as Principal Component 1 versus Principal Component 2 from the statistical analysis. Principal Component 1 is comprised of elements affected by basalt infiltration into the xenoliths, so the original sandstone formation plots within the outlined region to the left of the sandstone xenoliths. Principal Component 2 represents trace mineral heterogeneities in the original regional sandstone samples.

were sampled close to Mole Hill to minimize spatial variation. Although grain size and shape by themselves are not unique identifiers of the source horizon of the sandstone xenoliths at Mole Hill, these data can be used to help eliminate some possible sources of the sandstone xenoliths (Figure 4). In particular, the hydrothermal chert from within the contact zone at Mole Hill exhibits a range of grain sizes distinctly wider than the range observed in the sandstone xenoliths. This grain size distribution in conjunction with the distinct radial crystal habit of the chert makes the hydrothermal chert an unlikely candidate for the source of the sandstone xenoliths. Almost all of the framework grains in the sandstone xenoliths have a long axis to short axis ratio of <2.5, but about a third of the framework grains in sample of the Antietam have a long axis to short axis ratio of >2.5. Based on grain size and grain shape analyses, the Antietam Sandstone and the hydrothermal chert from Mole Hill seem unlikely to be the source of sandstone xenoliths.

The geochemical data also do not provide a uniquely distinct means to identify the source rock of the xenoliths. These data do restrict the source to four stratigraphic units: the Tuscarora Sandstone, Foreknobs Formation, the sandstone from the Conococheague Formation, or the hydrothermal chert at Mole Hill. The Oriskany and Massanutten Formations are possible but less plausible sources based on geochemistry, since some of the data for these units lie outside of the anticipated parent sandstone composition.

Another important consideration is whether or not there is a plausible structural mechanism for entraining each unit within the Mole Hill basaltic magma during its ascent through the crust. The chert in the contact zone is the most proximal to the magma, and presumably fragments of it would have been easily entrained if it had formed between pulses of magma. The Conococheague Sandstone is exposed just to the southwest of Mole Hill (Figure 1). The Tuscarora, Juniata, Oswego, and Keefer Formations are all exposed within horse blocks along the North Mountain Fault system. Regional stratigraphic and facies relations (Figure 2) make it unlikely that the Massanutten Sandstone, exposed along the eastern edge of the Shenandoah Valley and the stratigraphic equivalent to the combined Tuscarora and Keefer Formations, would be found at depth in the western Shenandoah Valley at Mole Hill. It is unlikely that the Swift Run, Antietam, Harpers, or Weverton Formations, exposed in the Blue Ridge, would be found in a pristine state in the western Shenandoah Valley. If these Cambrian and Precambrian units are present in the western Shenandoah Valley, they are most likely found in the lower duplex system (Figure 1) and would be expected to exhibit highly deformed textures if found as xenoliths in Mole Hill.

Both the Silurian Tuscarora Formation and the Devonian Oriskany Formation are exposed to the west of the North Mountain Fault, making them structurally more likely candidates than sandstone units exposed to the east. The Oriskany Formation is missing from the section of the North Mountain Fault closest to Mole Hill (Location 6, Figure 1). In contrast, the Tuscarora Formation is found as a breccia at Brocks Gap (Location 5, Figure 1) along the North Mountain Fault. After the Mole Hill magma ascended through fractures in the lower duplex and entered the North Mountain décollement (Figure 1), it was impeded by the Tuscarora Formation within the décollement. Clasts from the Tuscarora Formation could have been entrained within the Mole Hill magma as it exploded through the décollement and exploited a splay fault within the North Mountain duplex to reach the surface (Cross-section, Figure 1). Southworth and others (1993) proposed that Eocene dikes and intrusions in Highland County, VA, formed during extensional reactivation of preexisting structures including a NE-trending basement fracture zone and a cross-strike basement fracture zone. Unlike the interpretation in this work, Mesozoic and Eocene dikes are shown vertically cross-cutting structures in the upper crust (Southworth and others, 1993).

It is also possible that Mole Hill could be located along the surface expression of a lateral ramp similar to others within the Appalachians, including in Highland County (Pohn, 2000). Igneous intrusive swarms occur parallel to lateral ramp structures elsewhere in the Appalachian Orogeny (Pohn, 2000). The intersection of possible transform faults or fracture zones due to lateral motion parallel to the strike of the cross-section in Figure 1 with the shallow thrust splay of the North Mountain Fault seen in the cross-section (Pierce and Doctor, 2011) provided a convenient conduit for the Mole Hill magma.

CONCLUSIONS

The Silurian Tuscarora Formation is the most likely source for the sandstone xenoliths at Mole Hill based upon a combination of textural, grain size, compositional, and structural considerations. The Devonian Oriskany Formation has many characteristics similar to the Tuscarora Formation and sandstone xenoliths at Mole Hill. However, the Oriskany lacks pervasive linear to curvilinear inclusion tracks and well-developed quartz overgrowths on framework grains, its geochemistry does not completely fall within the projected protolith composition for the sandstone xenoliths at Mole Hill, and it is missing from the North Mountain Fault near Mole Hill.

Identification of the sandstone xenoliths at Mole Hill as the Silurian Tuscarora Formation or possibly the Devonian Oriskany Formation implies that these younger units extend underneath Mole Hill in the western Shenandoah Valley within the North Mountain Fault zone (cross-section A-A' in Figure 1). Previous interpretations of the cross-section underneath the western Shenandoah Valley (Evans, 1989; Southworth and others, 1993) terminate the wedge of Silurian and Devonian units within the footwall of the North Mountain Thrust to the west of Mole Hill.

Basaltic magma ascending through the crust underneath Mole Hill would first exploit the splay faults in the lower duplex (cross-section A-A' in Figure 1) to reach the décollement of the North Mountain Thrust Sheet. The Tuscarora Formation located within this zone was entrained in the basalt as it punctured through the fault zone and continued to the surface along existing thrust splays, perhaps at the edge of a lateral ramp produced during the Alleghanian Orogeny. The Mole Hill magma could have been temporarily entrapped within the North Mountain décollement, and the explosive force required for its continued ascent through secondary faults or fractures could explain why clasts of the Tuscarora Formation within the fault zone are the only likely crustal xenoliths found at Mole Hill. The Tuscarora represented the only significant structural barrier to magma ascent through the crust.

ACKNOWLEDGEMENTS

This research was supported by Grant J-984 from the Jeffress Foundation. Z. Kiracofe would like to thank the Tickle Foundation for providing fellowship money to support his undergraduate research in Summer 2011, and the JMU Materials Science Research Experience for Undergraduates (Grant DMR-085136 from the NSF and DoD ASSURE Program) for providing resources and travel money for this project. Z. Kiracofe and E. Johnson also thank the Virginia DMME (Matt Heller and Lorrie Coiner) for supplying samples and access to their geochemical database; Dan Doctor (USGS Reston) for help with sample collection and structural interpretation; Ron Phillips (JMU) for help in the laboratory; and Adam Wenger (JMU) for sample collection and GPS data at Mole Hill.

REFERENCES

Bartholomew, M.J., 1977, Geology of the Greenfield and Sherando quadrangles, Virginia: Virginia Division of Mineral Resources, Publication 4, 43 p.

Beard, J.S., 2010, Reconnaissance Mineralogy of the Eocene Mole Hill Diatreme, Rockingham County, Virginia: Jeffersoniana, v. 25, p. 1-16.

Campbell, E.V.M., Hibbitts, H.A., Williams, S.T., Duncan, I.J., Reis, J.S., Floyd, J.M., and Wilkes, G.P., 2006, Interstate 81 corridor digital geologic compilation: Virginia Division of Mineral Resources, Open File Report 06-01, scale 1:24000.

Evans, M.A., 1989, The structural geology and evolution of foreland thrust systems, northern Virginia: Geological Society of America Bulletin, v. 101, p. 339-354.

Furman, T. and Gittings, H, 2003, Eocene basalt volcanism in Central Virginia: implications for Cenozoic tectonism: Southeastern Geology, v. 42, p. 111-122.

Gathright, T.M., II and Frischman, P.S., 1986, Geology of the Harrisonburg and Bridgewater Quadrangles, Virginia: Virginia Division of Mineral Resources, Publication 60, 21 p.

Gathright, T.M., II, Henika, W.S., and Sullivan, J.L., II, 1977, Geology of the Waynesboro East and Waynesboro West Quadrangles, Virginia: Virginia Division of Mineral Resources, Publication 3, 53 p.

Herbert, P., Jr., and Young, R.S. (1956) Sulfide mineralization in the Shenandoah Valley of Virginia: Virginia Division of Geology, Bulletin 70, 58 p.

Hoffman, E.L., 1992, Instrumental Neutron Activation in Geoanalysis: Journal of Geochemical Exploration, v. 44, p. 297-319.

Pierce, H.A., and Doctor, D.H., 2011, Multi-resolution geophysical investigations and geologic mapping of a mantled karst aquifer, Briery Branch Quadrangle, Virginia, USA: Geological Society of America Abstracts with Programs, Paper No. 51-1.

Pohn, H.A., 2000, Lateral ramps in the folded Appalachians and in overthrust belts worldwide- A fundamental element of thrust-belt architecture: United States Geological Survey Bulletin 2163, 63 p.

Rader, E.K. and Evans, N.H., eds., 1993, Geologic map of Virginia – expanded explanation: Virginia Division of Mineral Resources, 80 p.

Rader, E.K. and Perry, W.J., Jr., 1976, Reinterpretation of the geology of Brocks Gap, Rockingham County, Virginia: Virginia Minerals, v. 22, p. 37-45.

Read, J.F.,1983, Field trip guide to Lower Paleozoic carbonate rocks, Roanoke region, Virginia: SEPM Eastern Section Meeting, VPI & SU, 31 p.

Roberts, W.P. and Kite, J.S., 1978, Syntectonic deposition of Lower to Middle Silurian sandstones, central Shenandoah Valley, Virginia: Virginia Minerals, v. 24, p. 1-5.

Sacco, B. and Johnson, E.A., 2011, Depth and temperature of the mantle beneath Mole Hill, an Eocene basalt near Harrisonburg, VA: Geological Society of America Abstracts with Programs, Paper No. 39-18.

Scherffius, W.E., 1969, Zinc-lead-fluorite mineralization of the Shenandoah Valley, north-central Virginia. Master's Thesis, Cornell University, p. 67-69.

Southworth, C.S., Gray, K.J., and Sutter, S., 1993, Middle Eocene intrusive igneous rocks of the central Appalachian Valley and Ridge Province- setting, chemistry, and implications for crustal structure: USGS Bulletin, Report B1839-I, p. J1-J24.

Tso, J.L. and Surber, J.D., 2006, Eocene igneous rocks near Monterey, Virginia: a field study: Virginia Minerals, v. 49, p. 9-24.

Wampler, J.M. and Dooley, R.E., 1975, Potassium-argon determination of Triassic and Eocene igneous activity in Rockingham County, Virginia: Geological Society of America Abstracts with Programs, v. 7, p. 547.

SOUTHEASTERN GEOLOGY
V. 49, No. 3, March 2013 p. 119-131

A NEW SPECIES OF *PROTOSCUTELLA* (ECHINOIDEA, CLYPEASTEROIDA, PROTOSCUTELLIDAE) FROM THE MIDDLE EOCENE (LUTETIAN) SANTEE LIMESTONE IN BERKELEY COUNTY, SOUTH CAROLINA

[1]ADAM S. OSBORN, RICH MOOI[2] AND [3]CHARLES N. CIAMPAGLIO

[1]1500 Lakeshore Drive, Camden, SC 29020 <macropneustes@netzero.com>
[2]Department of Invertebrate Zoology & Geology, California Academy of Sciences, 55 Music Concourse Drive, San Francisco, CA 94118 <rmooi@calacademy.org>
[3]Earth and Environmental Sciences, Wright State University – Lake Campus, 7600 Lake Campus Drive, Celina, OH 45822 <chuck.ciampaglio@wright.edu>

ABSTRACT

A new species of protoscutellid clypeasteroid sand dollar, *Protoscutella palmeri* n. sp., is described and discussed. Specimens were collected from a quarry near Jamestown, Berkeley County, South Carolina in which the mid-Eocene Santee Limestone is exposed. The new species occurs below the strata containing *Protoscutella mississippiensis mississippiensis* (Twitchell), which can be collected in the same quarry. The new *Protoscutella* is distinguished by a greatly widened (alate) test, yielding a width to length ratio much higher than that found in the subpentagonal to slightly elongated test of its congeners. Also unique among *Protoscutella*, the periproct of *P. palmeri* n. sp. is consistently and strongly supramarginal throughout ontogeny. Material was preserved well enough to present details of the oral plate pattern, and analysis of this pattern in several specimens reveals that there is some variation among individuals in terms of the disjunction of the interambulacral plate columns, but that there is consistency in the plate counts to the periproct. Protoscutellid sand dollars are important index fossils in the middle and upper Eocene of the Carolinas. *Protoscutella palmeri* n. sp. is no exception, being stratigraphically one of the earliest members of the family Protoscutellidae, and the earliest in the Carolinas.

INTRODUCTION

The genus *Protoscutella* Stefanini, 1924, presently includes six nominal taxa of relatively flat, discoidal, scutelliform (*sensu* Kroh and Smith, 2010) clypeasteroids belonging to a group colloquially referred to as sand dollars. Five species and one subspecies of *Protoscutella* have been described, including: *P. plana* (Conrad, 1865), *P. conradi* (Cotteau, 1891), *P. mississippiensis mississippiensis* (Twitchell in Clark and Twitchell, 1915), *P. tuomeyi* (Twitchell in Clark and Twitchell, 1915), *P. pentagonium* (Cooke, 1942), and the subspecies *P. mississippiensis rosehillensis* (Kier, 1980).

Protoscutella Stefanini, 1924, *Periarchus* Conrad, 1866, and *Mortonella* Pomel, 1883 are presently placed within the Protoscutellidae Durham, 1955. This clade, restricted to the Eocene of North America, is characterized by the presence of a fifth gonopore in the posterior interambulacrum. This feature has been characterized as a synapomorphy for the Protoscutellidae (Mooi 1987). All viable outgroups to the Protoscutellidae, notably other, possibly earlier Eocene forms, have four gonopores. Present views of the phylogenetic relationships within the Clypeasteroida strongly support the idea that a fifth gonopore has been derived independently in a small number of very distantly related clades, including protoscutellids.

Protoscutella is restricted to the middle Eocene of the Gulf Coast and Atlantic Coastal Plain of the southeastern United States, ranging as far west as Texas and as far north as North Carolina (Figure 1). Although phylogenetic relationships of taxa within the genus *Protoscutella* remain obscure, Durham (1955) and Mooi (1989) distinguished the genus from the other

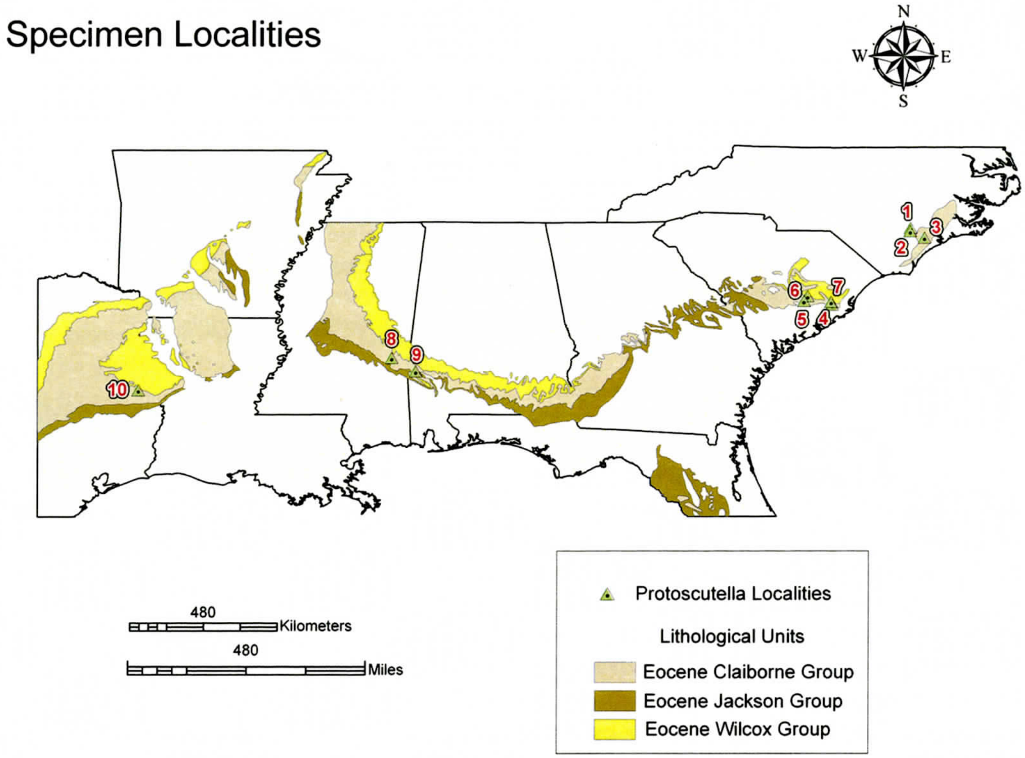

Figure 1. Outcrop zone of Eocene age strata in the Southeastern United States, with *Protoscutella* collecting localities mentioned within text annotated: 1) Well's Quarry, Rose Hill, Duplin Co., NC; 2) Fussel's Quarry, Rose Hill, Duplin Co., NC; 3) East Coast Quarry, Maple Hill, Pender Co., NC; 4) Martin Marietta Jamestown Quarry, *Protoscutella palmeri* n. sp., type locality, Jamestown, Berkeley Co., SC; 5) Wilson's Landing, Berkeley Co., SC.; 6) Martin Marietta, Orangeburg County Quarry, located directly across County Line Road from the now inactive Berkeley County Quarry, near Cross, Berkeley Co., SC; 7) Georgetown Quarry, now inactive, Georgetown Co., SC; 8) Type area of the type species of *Protoscutella*, *P. mississippiensis mississippiensis* (Twitchell), Chickasawhay River, Enterprise, Clarke Co., MS; 9) Valley of Souwilpa Creek, Choctaw Co., AL; 10) San Augustine, San Augustine Co., TX.

members of the Protoscutellidae, *Periarchus* and *Mortonella*, by its variably, but often discontinuous oral interambulacrum and straight, unbranched food grooves. Kier (1980) indicated that an interrupted posterior interambulacrum cannot be considered a unique feature of *Protoscutella*, as specimens of *Protoscutella conradi* (Cotteau, 1891) from Georgetown County, South Carolina, and Fussel's Quarry near Rose Hill, Duplin County, North Carolina (Figure 1) included specimens with a continuous posterior interambulacrum. Furthermore, Kier (1980) studied specimens that he identified as *Protoscutella plana* (Conrad, 1865) from Maple Hill, Pender County, South Carolina (Figure 1) with a continuous posterior interambulacrum. However, recent examination of Kier's material suggests Kier (1980) was incorrect in assigning the name *Protoscutella plana* to this material. Plate maps and other features of these specimens strongly suggest that these are actually members of the genus *Periarchus*.

Periproct position has been the key, and sometimes sole, feature used to distinguish the six nominal *Protoscutella* taxa accepted to date (Cooke 1959). Mooi (1989) tried to distinguish *Protoscutella* from *Periarchus* by its just submarginal periproct. Although the periproct is positioned closer to the margin in *Protoscutella* than in either *Periarchus* or *Mortonella*, a just submarginal periproct is not a consistent trait in the genus. In many specimens identified as *Protoscutella conradi* and *P. plana*, the periproct is far enough anterior to be considered firmly on the oral surface, and not at all associated with the posterior margin. This condition also applies to *P. pentagonium* and *P. tuomeyi*. *Protoscutella mississippiensis mississippiensis*, the type species of the genus, has a periproct that ranges from just submarginal, to slightly supramarginal. In juvenile specimens of *P. mississippiensis rosehillensis*, the periproct is typically situated directly on the margin or just supramarginally. Finally, in the new species described here, *P. palmeri* n. sp., the periproct remains strongly supramarginal throughout growth (see below).

Although there is clearly some value to periproct position as a systematic feature in *Protoscutella*, there is considerable variation among populations presently assigned to either *Protoscutella conradi* or *P. plana*. Even early results from a complete re-examination of all members of the genus, taking into account oral plate architecture and other characters, show that the commonly used, present nomenclature is widely divergent from the original descriptions and morphology of the types. It would appear that no one has consulted the types (actually lectotypes) of *P. plana* and *P. conradi* since their images were shown in Clark and Twitchell (1915), and this has caused much confusion in the nomenclature of the group. For example, as suggested above, it became apparent during our comparative analysis for *P. palmeri* n. sp. that Kier (1980) did not have the true *P. plana* in hand when he described and figured material he ascribed to that species, further underscoring the need for a complete revision of the genus, if not the entire family. Our access to type material of all the relevant species is resulting in a major revision of *Protoscutella* -- ongoing work that informs the present paper, but which will be published elsewhere.

GEOLOGIC SETTING

The specimens of *Protoscutella palmeri* n. sp. described herein were collected from the basal bryozoan biomicrudite, "lithozone 1a" of Banks (1977), of the mid-Eocene Santee Limestone within the Martin Marietta Quarry, southeast of Jamestown, Berkeley County, South Carolina (Figure 1). This horizon is equivalent to the Warley Hill Marl of the mid-Eocene Santee Limestone, residing in NP zone 15 in the Martin Marietta Quarry. Here, the new species occurs below its congener *P. mississippiensis mississippiensis*, from which it is easily distinguished (see below). We have found no specimens of *P. palmeri* n. sp., or any records of this distinct form, outside of the Jamestown Quarry where strata of equivalent age are mined in Berkeley, Dorchester, and Orangeburg Counties, South Carolina. The addition of *P. palmeri* n. sp., along with a new species of *Salenia* currently being studied by the authors, increases the number of echinoid species recorded from the Santee Limestone to 17 (Kier 1980, Powell and Baum 1982).

The horizon in which the *P. palmeri* n. sp. is found consists of a dense, pale gray, indurated bryozoan biomicrudite. Banks (1977) designated the *Cubitostrea lisbonensis* biozone as extending to the base of the Santee Limestone to include strata formerly referred to the Warley Hill Marl. This designation places *P. palmeri* n. sp. within the biozone of the oyster *C. lisbonensis* (Banks 1977, Baum et al. 1980), though specimens of *C. lisbonensis* were not collected from this horizon within this quarry. *Protoscutella palmeri* n. sp. occurs with a sparse echinoid assemblage consisting of rare, elongate specimens of *Santeelampas oviformis* (Conrad), *Cidaris pratti* (Clark) and an undescribed species of the genus *Salenia*. The authors are currently studying specimens of this elongate variant of *S. oviformis* (Conrad), as well as specimens of the genus *Salenia*. The latter represents the first occurrence of *Salenia* in the Eocene of North America. Other invertebrates are present, including abundant crab remains, the nautiloid *Aturia*, and a rich fauna of bryozoans

Table 1: Measurements of *Protoscutella palmeri* n. sp. All measurements are in millimeters. * denotes approximation based on reconstruction, dash means measurement was not made due to matrix or damage. L = length (mm), W = width (mm).

Specimen	L	W	L as %of W	Petaloid I L	Petaloid II L	Petaloid III L	Peristome W	Periproct W	Periproct to posterior margin	# Pores in one column of petaloid I	# Pores in one column of petaloid II	# Pores in one column of petaloid III
Holotype UF 213520	39.3	55*	140	10.1	9.6	10.6	2.5	1.5	2.5	48	47	48
Paratype UF 213521	29.1	34.4	118	7.4	—	7.4	2.3	1.4	1.8	—	—	36
Paratype UF 213522	38.5	—	—	—	—	—	2.7	—	—	—	—	—
Paratype UF 213523	26.8	33.6	125	—	—	—	2.0	1.0	1.8	—	—	—
Paratype UF 213524	28.9	34.9	121	—	—	—	—	1.2	1.8	—	—	—
Paratype UF 213525	20.6	22.8	111	—	—	—	1.6	—	—	—	—	—
Paratype ASG 72081	29.0	37.6	130	—	—	—	1.9	—	—	—	—	—
Paratype ASG 72082	33.9	43.9	129	—	—	—	1.8	—	—	—	—	—
B. Palmer Collection	29.3	39.1	133	7.5	7.4	7.7	—	1.4	1.9	35	—	—
A. Osborn Collection	51.5	81.6	158	—		—	3.7	—	—	—	—	—

and small bivalves.

The *in situ* fossiliferous deposit is not directly accessible because the quarry is water-filled. Mining operations consist of dredging limestone from beneath the water and blocks of this horizon are brought up from the deepest portions of the quarry along the quarry perimeter. Excavations containing blocks of the *P. palmeri*-bearing basal Santee Limestone horizon also contain sediment from an underlying zone of glauconitic limestone with a rich fossil vertebrate fauna. This fauna was discussed by Cicimurri and Knight (2009), and based on the vertebrate and invertebrate fauna of this unit, they speculated that this horizon represents an unnamed lower Eocene, Ypresian deposit which unconformably underlies the Santee Limestone in the Jamestown Quarry.

The presence of this material mixed in the dredges with the basal Santee Limestone blocks, which contain the remains of *P. palmeri* n. sp., helps secure the placement of this sand dollar within the stratigraphic succession of this quarry. A less indurated horizon of limestone with a rich mollusk and crab fauna overlies the zone containing *P. palmeri* n. sp. This horizon harbors the two characteristic echinoid species of the *Cubitostrea lisbonensis* biozone, *Santeelampas oviformis* and *P. mississippiensis*, as well as *Eurhodia baumi* (Kier). In turn, this horizon is overlain by lithozone II of the Santee Limestone (Banks 1977), and the *Cubitostrea sellaeformis* (Conrad) biozone of the Santee Limestone (Baum et al., 1980), which contains the aforementioned echinoids *Cidaris pratti* and *P. conradi*, as well as *Eurhodia rugosa rugosa* (Ravenel), *Eurhodia holmesi* (Twitchell), and *Linthia hanoverensis* (Kellum).

Cooke and MacNeil (1952) erected the Warley Hill Marl to include glauconitic sands containing the oyster *Cubitostrea lisbonensis*. However, Banks (1977) included this unit within the Santee Limestone, as the lithofacies of both were similar. Baum et al. (1980) proposed the abandonment of the term Warley Hill Marl in favor of the *Cubitostrea lisbonensis* and overlying *Cubitostrea sellaeformis* biozones of the Santee Limestone. Geisler et al. (2005) pro-

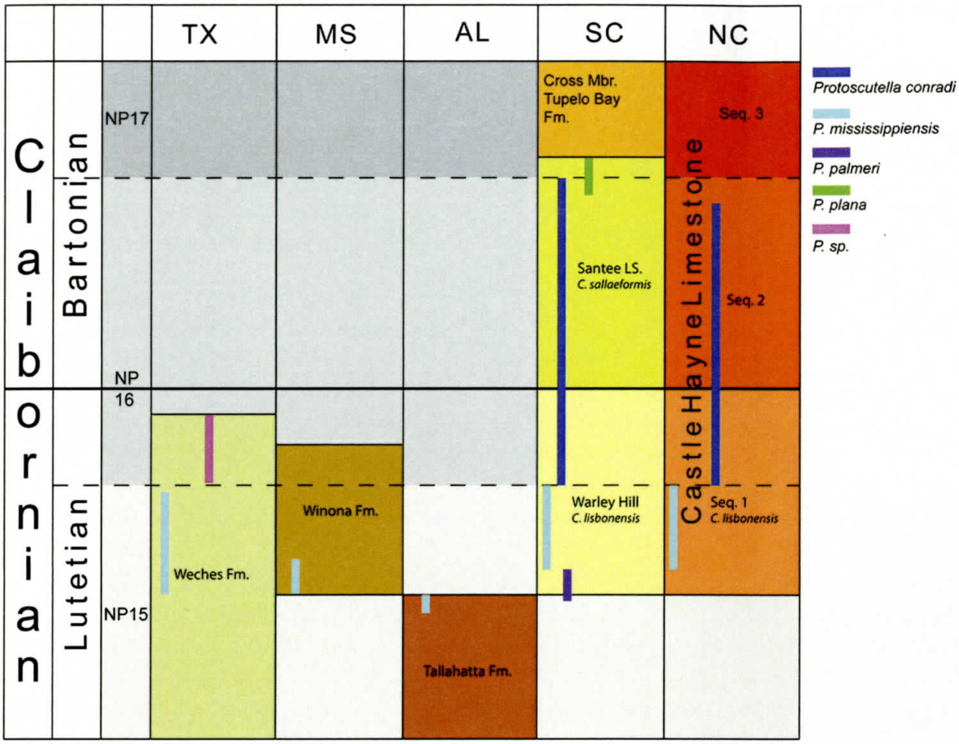

Figure 2. Generalized correlation chart of significant *Protoscutella*-bearing units displaying distribution of *Protoscutella* species. Correlation and *Protoscutella* distribution follows Baum and Vail (1988), Geisler et al. (2005), Toulmin (1977), Zachos and Molineaux (2003), and Zullo and Harris (1987). Note that the *P. palmeri*-bearing NP15 limestone in the Jamestown Quarry is herein treated as the basal Santee Limestone, age equivalent of the Warley Hill Formation. Precise placement of *P. palmeri* within the unit is uncertain. Additionally, examination of type material of both *P. conradi* and *P tuomeyi* undermines the designation of *P. conradi* for specimens documented from the Weches Formation of Texas by Zachos and Molineux (2003). We here designate these specimens as *Protoscutella* sp., pending further study. Furthermore, new data from field work that will soon be reported upon has uncovered *P. conradi* occurring *in situ* with *P. plana* in the lower bed of their distribution in Orangeburg Co., SC. This observation is also reflected in the chart.

posed restricting the name Santee Limestone to the strata of NP 16 age underlying the Tupelo Bay Formation, and reviving the Warley Hill Formation to occupy the portion of the Santee Limestone that resides beneath zone NP16. If the redesignations proposed by Geisler et al. (2005) are accepted, the basal limestone containing *P. palmeri* n. sp. in the NP 15 zone would be "technically" designated as the Warley Hill Formation, though it is lithologically more similar to the overlying limestone of the *Cubitostrea sellaeformis* zone than the typical glauconitic sandy marl of the Warley Hill Formation.

The original type locality of the Santee Limestone at Eutaw Springs, Orangeburg County, South Carolina now lies beneath the waters of Lake Marion, created in the 1940s after the damming of the Santee River. Although Geisler et al. (2005) suggested Eutaw Springs should still be recognized as the type area for the Santee Limestone, as other outcrops of the Santee Limestone can be viewed in the area, the formation is best viewed in South Carolina within a series of quarries in Berkeley, Dorchester, and Orangeburg Counties. Within these quarries the Santee Limestone is overlain by an upper-middle Eocene age bryozoan-brachiopod-bivalve biomicrite formerly referred to as the Cross Member of the Santee Limestone (Ward et al. 1979). Geisler et al. (2005) proposed the name "Tupelo Bay Formation" for the strata that were formerly included within the Cross Member of the Santee Limestone, and proposed limestone from depths 189.4 to 90.9 feet of the USGS Pregnall Core (Edwards et al. 1997), Dorchester County, South Carolina, as the type section for the Tupelo Bay Formation.

The Santee Limestone was deposited in open, warm, clear waters of normal marine salinity, free of terrigenous sediment and similar to current-day subtropical to tropical environments (Banks 1977). Gardner (1957) proposed a maximum depth of 50 m for the *Cubitostrea lisbonensis* zone, while Banks (1977) surmised the limestones were deposited on a sublittoral, offshore open shelf, in waters less than 100 m deep.

To summarize, at the Jamestown Quarry, Berkeley Co., South Carolina (Figure 1), the Santee Limestone consists of a lower portion (Warley Hill Formation equivalent), that contains *Protoscutella palmeri* n. sp. This lower portion lies beneath a limestone horizon containing species characteristic of the *Cubitostrea lisbonensis* biozone of NP zone 15. The unit is underlain by an Ypressian age, unnamed, vertebrate-rich, glauconitic deposit (Cicimurri and Knight, 2009).

SYSTEMATIC PALEONTOLOGY

Figured specimens are deposited with the Invertebrate Paleontology Division, Florida Museum of Natural History at the University of Florida (UF), and at the California Academy of Sciences, San Francisco (CASG). The classification follows Kroh and Smith (2010).

Class ECHINOIDEA Leske, 1778

Order CLYPEASTEROIDA L. Agassiz, 1835

Suborder SCUTELLINA Haeckel, 1896

Family PROTOSCUTELLIDAE Durham, 1955

Type genus *Protoscutella* Stefanini, 1924

Type species *Protoscutella mississippiensis mississippiensis* (Twitchell in Clark and Twitchell, 1915)

Protoscutella palmeri new species (Figures 3 - 5)

Diagnosis: Test significantly expanded laterally (alate, *sensu* Mooi et al., 2000), much more so than in any other species of *Protoscutella*. Test width increases significantly in proportion to the test length as the specimens increase in size so that the test has a distinct triangular shape as the test widens through the posterior paired interambulacra. Periproct conspicuously supramarginal in both small and large specimens. First plates to contact the periproct moving distally from the peristome are the a7 and b7 plates, as identified using the Lovénian system (Lovén, 1874).

Description: Test medium to large, largest specimen with complete margin (not in type series): L = 51.5 mm; W = 81.6 mm; width being 158% of length, smallest specimen: L = 20.6 mm; W = 22.8mm; width being 111% of length (table 1). Outline subpentagonal in juvenile specimens, becoming progressively laterally elongate with increasing size (Figures 3 and 4). Mature specimens distinctly triangular, widest points occurring at intersection of line drawn orthogonally to anterior-posterior axis through posterior paired interambulacra (Figure 4), about half-way between apical system and posterior margin of test. Margin thin, posterior margin with distinct anal notch and slight indentations where ambulacra 1 and 5 form the ambitus, indentations more pronounced with increased size (Figures 3 and 4).

Aboral surface slightly tumid, highest at apical system. Apical system central with five genital pores and large central madreporite containing scattered hydropores not associated with grooves *sensu* Mooi (1989) (Figure 5).

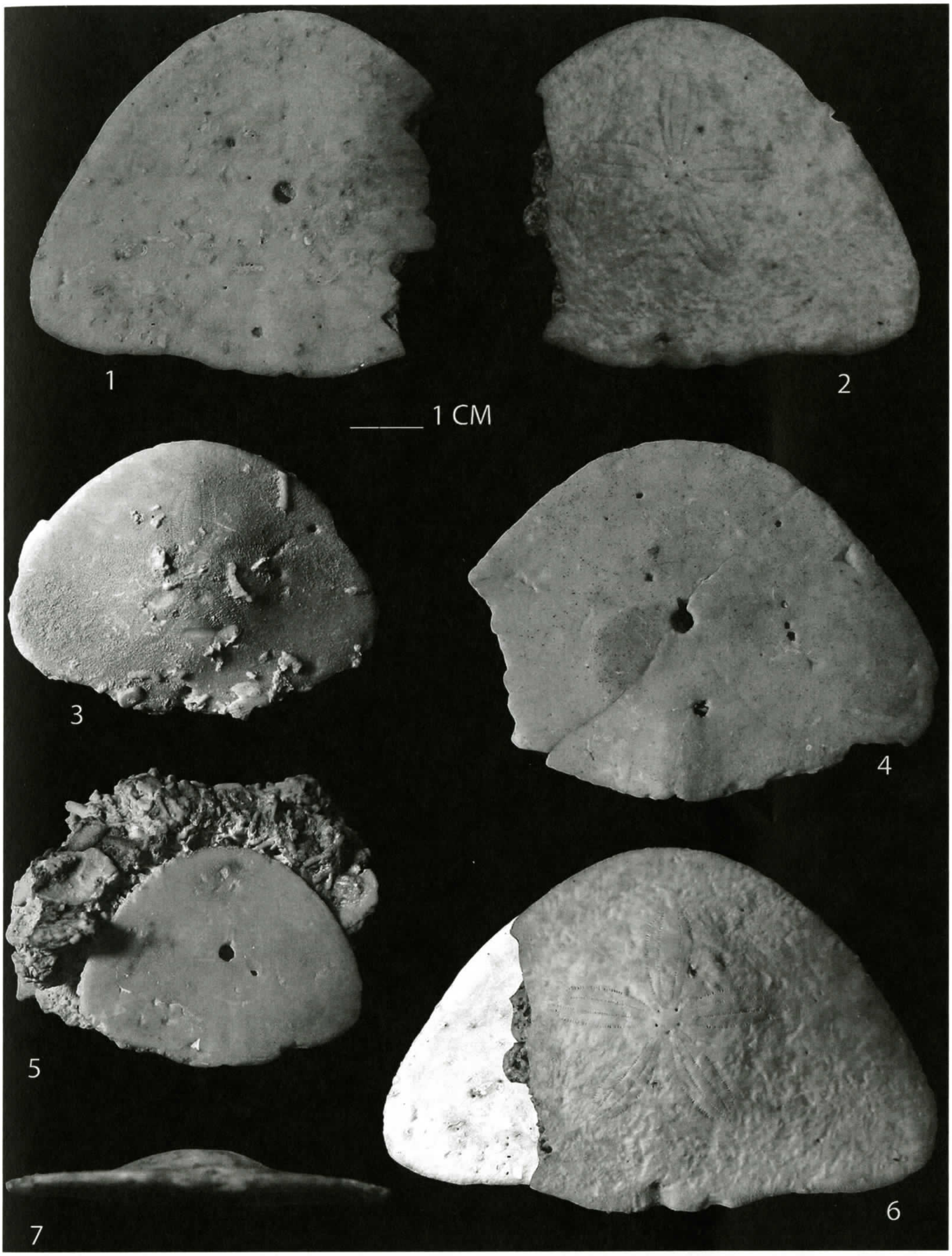

Figure 3. ***Protoscutella palmeri*, n. sp., Santee Limestone, Jamestown Quarry, Jamestown, Berkeley County, South Carolina. Anterior unpaired ambulacrum (ambulacrum III) at top of each image. 1: Holotype, UF 213520, oral surface. 2: Holotype, UF 213520, aboral surface. 3: Paratype, UF 213521, aboral surface. 4: Paratype, UF 213522, oral surface. 5: Paratype, UF 213523, oral surface. 6: Holotype, UF 213520, aboral surface with reconstructed left side. 7: Paratype, UF 213524, left lateral view.**

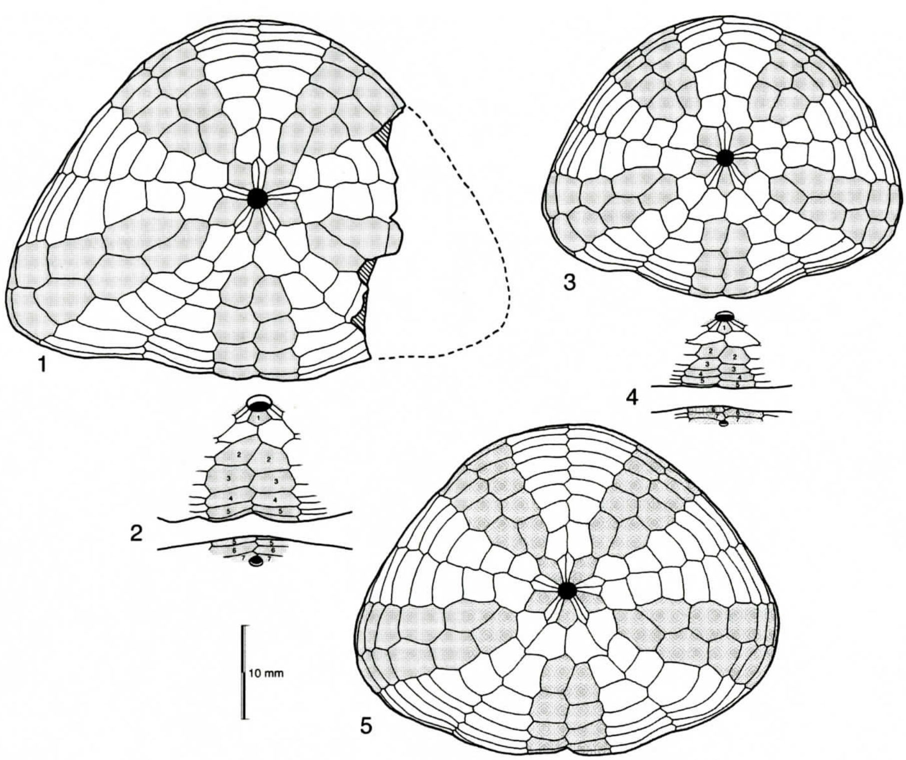

Figure 4. Plate maps of the oral surface and periproct positions for *Protoscutella palmeri* n. sp. Interambulacral plates are shaded, peristome and periproct are filled in black, damaged areas cross-hatched. Plates in the posterior interambulacrum numbered according to the Lovénian system. Anterior unpaired ambulacrum (ambulacrum III) towards top of each image. All images to same scale. 1: Holotype, UF 213520, oral surface with reconstructed left side. 2: Holotype, UF 213520, 2 successive, oblique views at increasing angles around the ambitus showing plating up to the aboral periproct. 3: Paratype, CASG 72081, oral surface. 4: Paratype, CASG 72081, 2 successive, oblique views at increasing angles around the ambitus showing plating up to the aboral periproct. 5: Paratype, CASG 72082, oral surface

Petaloids lanceolate, headed by small but distinct ocular plate containing an ocular pore (Figure 5). Petaloids slightly closed distally with 2 or 3 trailing podia (*sensu* Mooi 1989). Distal plates of petaloid do not typically appear to be occluded from contact with adjacent interambulacral plates in most cases (Figure 5), but this occlusion does seem to occur in only one or two instances in one of the paratypes (UF 213521). Petaloids approximately same length, equal to 25-26% of test length (Figures 3, 5; Table 1). Petaloid in ambulacrum III extends on average 60% distance from apex to margin, but in ambulacra I, II, IV, V, petaloids extend on average 50% of distance from apical system to corresponding ambitus. Pore pair counts (not counting the trailing podia) for a single column of respiratory pores in ambulacra I, II, and III are shown in Table 1 for specimens in which the aboral surface is visible. Accessory pores present in interporiferous zone of petaloids, scattered in plates distal to petaloids and approaching the ambitus. Interambulacra are zig-zag biserial all the way to apical system (Figure 5). Aboral spine tubercles small, densely packed as typical for most scutellines, differentiated into primary and miliary (*sensu* Mooi 1986).

Periproct strongly supramarginal, ovate, slightly longer than wide, diameter equal to 3.8 - 4.9% test length, positioned in slight groove on aboral surface on average 6% of test length from posterior margin. Oral surface flat with slightly raised (keeled) region extending from posterior marginal notch towards peristome, becoming flush with oral surface about 1/3 of distance from margin to peristome. Pressure drainage channels (*sensu* Mooi 1989) absent. Peristome central, 6.3-7.9% of test length. Basicoronal plates star-shaped, interambulacral plates much larger than ambulacral, almost twice as long (Figure 4). In holotype and two paratypes for which complete oral surface plate maps were obtained, paired interambulacra (interambulacra 1, 2, 3, and 4) were variably disjunct (Figure 4). However, posterior interambulacrum (interambulacrum 5) always disjunct, with first post-basicoronals widely separated from corresponding basicoronal. Main branch of food grooves extending to distal part of second post-basicoronals in each oral ambulacrum. Distal to this point are faint traces of bifurcation barely detectable in some ambulacra of some specimens where absence of tubercles and slight elongation of podial pores delineate short, simple branch onto each column of more distal interambulacral plates. Apparent extension of main branch of groove to ambitus seen in Figure 3 is result of artifact or preparation. Center of unbranched part of food groove occupied by sharply defined keel flanked by food groove podial pores. Proximal portion of keel slightly swollen where it passes over sphaeridial chamber, in which single, glassy sphaeridium is present in well-preserved specimens. Keel produced into small point directed into peristome, with buccal podial pores flanking this point just inside peristome relative to point. Little or no differentiation of tubercles into ambulacral versus interambulacral locomotory fields. Tubercles only slightly larger than those on aboral surface.

Internal peripheral buttressing and pillars well-developed, but not thickened or heavy. Lantern supports consist of single auricles, one per interambulacral basicoronal. Lantern structure unknown.

Material: Holotype UF 213520, and paratypes: UF 213521 - 213525, CASG 72081 – 72083, all collected from the Santee Limestone, Jamestown Quarry, Berkeley County, South Carolina. Measurements for examined specimens are given in Table 1.

Etymology: This species is named in honor of Bill Palmer, collector of many of the studied specimens.

Occurrence: *Protoscutella palmeri* n. sp. has not been documented outside of Berkeley County, South Carolina where it is found in the basal horizon of the mid-Eocene Santee Limestone in the Martin Marietta Quarry, Jamestown, South Carolina (Figures 1 and 2).

Discussion: *Protoscutella palmeri* n. sp. is most similar to *Protoscutella mississippiensis mississippiensis* (Twitchell), but is readily differentiated by its greatly exaggerated width to length ratio and the consistently aboral position of its periproct. The smallest measured specimen has a width to length ratio of 111%, whereas the largest studied specimen has a width to length ratio of 158% (Table 1).

Kier (1980) stated that specimens of *P. mississippiensis mississippiensis* from the Winona Formation at the type locality near Enterprise, Mississippi have a width that is on average 103.7% of the test length, and specimens of *P. mississippiensis mississippiensis* from Wilson's Landing, near Eadytown, Berkeley County, South Carolina, have a width on average 107% of test length. However, specimens of *P. mississippiensis mississippiensis* from the Santee Limestone within the Jamestown quarry above the occurrence of *P. palmeri* n. sp. have a width that is on average only 99% of test length. *P. mississippiensis rosehillensis* from the type locality near Rose Hill, Duplin County, North Carolina, have a width on average 100.4% of test length. Zachos and Molineaux (2003) stated that large specimens of *P. mississippiensis mississippiensis* from the Weches Formation of Texas have widths that range from 110-125% test length, but it appears that the very highest width to length ratios of this population are not common or typical, nor does it result in the alate, or slight triangular outline of the test seen in even the smallest known *P. palmeri* n. sp.

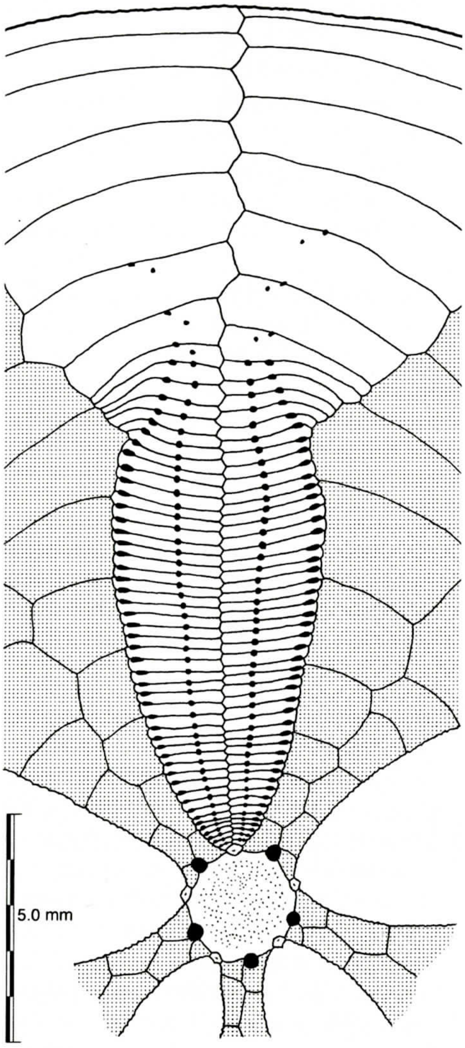

Figure 5. Plate map and pore patterns of the apical region and ambulacrum III for *Protoscutella palmeri* n. sp., Holotype, UF 213520. Interambulacral plates are shaded, pores are filled in black, details of ambulacral plating in interambulacra 1, 2, 4, and 5 omitted, accessory pores in interporiferous zone and distal ambulacral plates present, but not shown.

The width to length ratio of the test of *P. palmeri* n. sp. increases significantly as the specimens increase in size (Table 1, Figures 3 and 4). The point of greatest width of *P. palmeri* n. sp. is significantly more posterior than in other species of *Protoscutella*. Juvenile specimens of *P. palmeri* n. sp. have a point of greatest width that is adjacent to, or just posterior of the apical system, which is similar to other species of *Protoscutella* which typically have a point of greatest width that is central or just posterior of center. However, as individuals of *P. palmeri* n. sp. increase in size, the point of greatest width progressively becomes more posterior, eventually to become situated more than 50% of the distance from the apical system to the posterior margin. The effect of this is to produce a very distinctive triangular outline in the largest individuals (Figures 3, 4).

Protoscutella palmeri n. sp. is also readily differentiated from all other protoscutellid species by the consistently aboral position of its periproct. All other Protoscutellidae have submarginal or distinctly oral periprocts with the exception of *P. mississippiensis*, in which the periproct is variably placed, ranging from marginal to just barely supramarginal. Specimens from the Winona Formation in the type area of Enterprise, Mississippi and from the Weches Formation in Texas have a periproct that is just submarginal in large specimens, and marginal in small specimens. *P. mississippiensis mississippiensis* from Wilson's Landing, South Carolina and specimens of the subspecies *P. mississippiensis rosehillensis* from North Carolina have a periproct that is just supramarginal in small specimens, but it becomes more marginal in larger individuals (Kier 1980). The periproct placement of *P. palmeri* n. sp. is most similar to, though distinctly different from, the marginal to just supramarginal periproct of the Tallahatta Formation population of *P. mississippiensis mississippiensis*, in the valley of Souwilpa Creek, Choctaw County, Alabama. However, three of eight examined specimens of the Souwilpa Creek population had marginal periprocts. Of the five specimens with just supramarginal periprocts, the distance of the periproct above the margin is on average merely 1.8% of test length. In *P. palmeri* n. sp., the periproct is at a distance of 6.1 - 6.6% of test length above the posterior margin. The periproct on specimens in the Tallahatta Formation is situated in an anal notch, and though the periproct is visible from above, the periproct is also clearly visible when viewing the test from the posterior margin. The periproct of *P. palmeri* n. sp., being positioned further from the margin on the aboral surface, is not typically visible from a marginal aspect.

Data from plate maps across all taxa of protoscutellids (personal observation) suggest that the degree to which the interambulacra are disjunct from the basicoronals on the oral surface is a key taxonomic feature. However, *P. palmeri* n. sp. is somewhat enigmatic in this regard due to the variation seen in the three specimens for which these data are available. In all specimens, the posterior, unpaired interambulacrum (interambulacrum 5) is disjunct, which is a feature seen in a variety of other *Protoscutella* species, including *P. mississippiensis*, some specimens of *P. conradi*, the type and only known specimen of *P. pentagonium*, and all specimens that can be assigned unambiguously to *P. plana*. In two of the *P. palmeri* n. sp., the anterior paired interambulacra (interambulacra 2 and 3) are continuous by contact between the basicoronals with only one of the two corresponding post-basicoronals (Figure 4). The posterior paired interambulacra (interambulacra 1 and 4) are disjunct in all specimens, except for slight contact by one of the post-basicoronals in the holotype (Figure 4). In almost all *Protoscutella* species for which preliminary data exist, the larger the specimen, the more likely that some disjunction will occur. However, in *P. palmeri*, the smallest of the specimens examined for oral plate mapping shows the highest degree of disjunction, furthermore in all five of the interambulacra. The significance of this variation has yet to be related to phylogenetic, ontogenetic, or environmental factors, or to phenotypic plasticity that might influence disjunction in other species of *Protoscutella*. It is likely that additional data from other specimens of the new species will shed light on these questions, particularly if complete surveys of plate patterns can be made for all valid taxa in the family.

The apparent succession of species of *Protoscutella* has been given great importance because the members of the genus are regarded as important index fossils for the middle Eocene faunal zones of the Carolinas (Kier 1980, Zullo and Harris 1987). As suggested by Zachos (2009), the relative stratigraphic positions of protoscutellid taxa from *P. mississippiensis* to *P. conradi* (to *P. plana* in South Carolina), followed by *Periarchus lyelli*, is consistent throughout their range without regard to sediment type. The specimens are found within clastics in the Gulf Coastal Plain and carbonates in North and South Carolina. With the addition of *P. palmeri* n. sp. to the genus, the sequence of taxa in South Carolina is now modified to include *P. palmeri* n. sp. as the earliest species for the region (Figure 2).

The earliest protoscutellids known from the Gulf Coast region belong to a population of *P. mississippiensis* occurring with *Cubitostrea perplicata* (Dall), at the top of the Tallahatta Formation in the valley of Souwilpa Creek, Choctaw County, Alabama (Figure 1). It is likely that this occurrence of *P. mississippiensis* predates that of *P. palmeri* n. sp. Banks (1977) used the biostratigraphic correlation of Toulmin (1969) and the presence of *Cubitostrea lisbonensis* (Harris) to correlate lithozone 1 of the Santee Limestone (equivalent of the Warley Hill Marl of Cooke and MacNeil [1952]) with the middle Eocene, lower Lisbon Formation of Alabama. This correlation suggests that *P. mississippiensis* (Twitchell) from the *C. perplicata* (Dall) zone in the upper Tallahatta Formation, just below the contact with the Lisbon Formation, is older than the population of *P. palmeri* n. sp. discussed within this paper, making the Tallahatta sand dollars the oldest documented population of *Protoscutella* (Figure 2). However, at Enterprise, Mississippi (Figure 1), near the type locality of *P. mississippiensis*, both *C. lisbonensis* and *C. perplicata* occur in the Winona Formation with *P. mississippiensis* (Dockery 1980). It can be concluded that using oyster biozonation to correlate these strata is imperfect (Zullo and Harris 1987). It is also notable that *C. lisbonensis*, which is known to occur with *P. mississippiensis* above *P. palmeri* n. sp. in the Santee Limestone, does not appear in the basal limestone bed with *P. palmeri* n. sp. in the Jamestown, South Carolina quarry. Therefore, the horizon containing *P. palmeri* n. sp. within the Jamestown Quarry could reside beneath the

Cubitostrea lisbonensis horizon, and its relationship to the population of *P. mississippiensis* at the top of the Tallahatta Formation would then be in question. The Eocene stratigraphy of South Carolina has been a topic of much debate amongst regional geologists, and until a consensus is reached, the authors are unable to make a determination on the aforementioned correlations. The relationship between the ages of these two populations remains an area for further study, though the relative positions of the Protoscutellidae in the Carolinas is now clear, from oldest to youngest: *P. palmeri* n. sp., *P. mississippiensis*, *P. conradi*, *P. plana*, and *Periarchus* (Figure 2).

The extreme widening of the test in *P. palmeri* n. sp. is reminiscent of eoscutellids, but it is premature to suggest through outgroup comparison that this feature of *P. palmeri* must be plesiomorphic for protoscutellids in general. This is not to say that the Eoscutellidae should not be considered a candidate outgroup for analysis of cladistic relationships within the Protoscutellidae, especially given the fact that both taxa evolved in the Eocene and are most likely to turn out to be basal to the rest of the scutelliforms (contrary to Kroh and Smith 2010). *Protoscutella palmeri* n. sp. is better regarded as providing evidence that specialized forms existed among the protoscutellids very early in the radiation of the group, and that widening of the test was an independent derivation of a mechanism to enhance feeding efficiency as suggested by Mooi et al. (2000).

Phylogenetic placement of *P. palmeri* n. sp. and its relationship to the stratigraphic occurrences of all species in the genus will provide significant understanding of the pattern of evolution and origins of novel traits among the Eocene clypeasteroids. Revisions of the taxonomy of these taxa, along with better understanding of their cladistic relationships could also lead to reinterpretations of the stratigraphy in North and South Carolina of strata for which protoscutellids are indicators and indices for correlation. Already, the unusual features of taxa such as *P. palmeri* n. sp. are posing questions that challenge previous understanding of these correlations, many of which are already not well understood.

ACKNOWLEDGEMENTS

We thank Bill Palmer for his specimen contributions, and comments concerning the geology and fauna of the Santee limestone in Berkeley County, South Carolina. His experience and knowledge gained from innumerable hours spent collecting the Santee Limestone were critical in the development of this manuscript. We also thank Dave Cicimurri for his insight on the stratigraphy of the Santee Limestone, and Adam Armstrong for providing a specimen of *Protoscutella palmeri* n. sp., for study and deposit as a paratype. The authors also wish to thank Vic Wright for preparing many of the paratypes from their ridiculously stubborn matrix. The authors are also indebted to the Martin Marietta Corporation, and their quarry managers who graciously allowed the collection of fossils from their quarries. We extend special appreciation to Mr. Handsome Major, of the Jamestown Quarry, for without his cooperation, *Protoscutella palmeri* n. sp. would remain undocumented. We are also indebted to Don Clements of Rocky Point, North Carolina, for providing specimens of North Carolina *Protoscutellids* for study from his extensive collection. We thank George Phillips, Lou Zachos and Roger Portell for their thorough and constructive reviews which greatly improved this manuscript.

REFERENCES CITED

Agassiz, L. 1835. Prodrome d'une monographie des Radiaires ou Echinodermes. *Memoires de la Société des Sciences Naturelles de Neuchatel*, 1: 168-199.

Banks, R.S. 1977. Stratigraphy of the Eocene Santee Limestone in three quarries of the coastal plain of South Carolina. *Geologic Notes, South Carolina Geological Survey*, 21(3): 1-149.

Baum, G.R., Collins, J.S., Jones, R.M., Madlinger, B.A., and Powell, R.J. 1980. Correlation of the Eocene strata of the Carolinas. *South Carolina Geology*, 24(1): 19-27.

Baum, G.R., and Vail, P.R. 1988. Sequence stratigraphic concepts applied to Paleogene outcrops, Gulf and Atlantic Basins. Pp. 309-327 in: *Sea-Level Changes—an Integrated Approach*, SEPM Special Publication No. 42.

Cicimurri, D.J., and Knight, J.L. 2009. New record of an extinct fish, *Fisherichthys folmeri* Weems (Osteichthyes), from the lower Eocene of Berkeley County, South Carolina, USA. *PaleoBios*, 29(1): 24-28.

Clark, W.R., and Twitchell, M.W. 1915. The Mesozoic and Cenozoic Echinodermata of the United States. *United States Geological Survey Monograph* 54, 341p.

Conrad, T.A. 1865. Descriptions of new species of Echinidae. *Proceedings of the Academy of Natural Sciences of Philadelphia*, 17: 75.

Conrad, T.A. 1866. Check list of the invertebrate fossils of North America: Eocene and Oligocene. *Smithsonian Miscellaneous Collections*, 7(200): 1-41.

Cooke, C.W. 1942. Cenozoic irregular echinoids of the eastern United States. *Journal of Paleontology*, 16(1): 1-62.

Cooke, C.W. 1959. Cenozoic echinoids of eastern United States. *United States Geological Survey Professional Papers*, 321: 1-106.

Cooke, C.W., and MacNeil, F.S. 1952. Tertiary stratigraphy of South Carolina. *United States Geological Survey Professional Papers*, 243-B: 1-29.

Cotteau, G.H. 1891. *Sismondia conradi*. In: Cotteau, G. H. 1889-1894. Terrain Tertiaire, Tome II. Échinides Éocènes. Familles des Cassidulidées (pars), Conoclypéidées, Clypéasteroidées, Scutellidées, Scutellinidées, Fibularidées et les Échinides réguliers. Paléontologie Française ou description des fossiles de la France continuée par une réunion de paléontologistes sous la direction d'un comité spécial, 1re Série. - Animaux Invertébrés G. Masson, Paris, 789 pp.

Dockery, D.T. III. 1980. The invertebrate macropaleontology of the Clark County, Mississippi Area. *Mississippi Department of Natural Resources Bureau of Geology Bulletins*, 72: 1-387.

Durham, J.W. 1955. Classification of clypeasteroid echinoids. *University of California Publications in Geological Sciences*, 31: 73-198.

Edwards, L.E., Bybell, L.M., Gohn, G.S., and Frederiksen, N.O. 1997. Paleontology and physical stratigraphy of the USGS-Pregnall no. 1 core (DOR-208), Dorchester County, South Carolina. *United States Geological Survey Open File Reports*, 97-145: 1-35.

Gardner, J. 1957. Little Stave Creek, Alabama-Paleontological Study. *Geological Society of America Memoirs*, 67: 573-588.

Geisler, J.H., Sanders, A.E., and Zhe-Xi Luo. 2005. A new protocetid whale (Cetacea: Archaeoceti) from the late middle Eocene of South Carolina. *American Museum Novitates*, 3480: 1-65.

Haeckel, E.H.P.A. 1896. Systematische phylogenie Entwurf eines natürlichen Systema der Organismen auf Grund ihrer Stammesgeschichte. *Th. II. Systematische Phylogenie der Wirbellosen Thiere (Invertebrata)*, Berlin. 720 p.

Kier, P.M. 1980. The echinoids of the middle Eocene Warley Hill Formation, Santee Limestone and Castle Hayne Limestone of North and South Carolina. *Smithsonian Contributions to Paleobiology*, 39: 1-102.

Kroh, A. and Smith, A.B. 2010. The phylogeny and classification of post-Palaeozoic echinoids. *Journal of Systematic Palaeontology*, 8(2): 147-212.

Leske, N. G. 1778. Additamenta ad Jacobi Theodori Klein naturalem dispositionem Echinodermatum et lucubratiunculam de aculeis echinorum marinorum. Lipsiae, Leipzig, 278 pp.

Lovén, S. 1874. Études sur les échinoïdées. *Kongliga Svenska Vetenskaps Akademiens Handlingar*, 11: 1-91.

Mooi, R. 1986. Structure and function of clypeasteroid miliary spines (Echinodermata, Echinoides). *Zoomorphology*, 106: 212-223.

Mooi, R. 1987. A cladistic analysis of the sand dollars (Clypeasteroida: Scutellina) and the interpretation of heterochronic phenomena. University of Toronto, Canada Ph.D. Thesis, 204 pp.

Mooi, R. 1989. Living and fossil genera of the Clypeasteroidea (Echinoidea: Echinodermata). An illustrated key and annotated checklist. *Smithsonian Contributions to Zoology*, 488: 1-51.

Mooi, R., Martínez, S., and Parma, S.G. 2000. Phylogenetic systematics of Tertiary monophorasterid sand dollars (Clypeasteroida: Echinoidea) from South America. *Journal of Paleontology*, 74(2): 263-281.

Pomel, A. 1883. Classification méthodique et genera des Échinides vivantes et fossiles. Thèses présentées à la Faculté des Sciences de Paris pour obtenir le Grade de Docteur des Sciences Naturelles 503, Adolphe Jourdan, Alger, 131 pp.

Powell, R.J., and Baum, G.R. 1982. Eocene biostratigraphy of South Carolina and its relationship to Gulf Coastal Plain zonations and global changes of coastal onlap. *Geological Society of America Bulletins*, 93: 1099-1108.

Stefanini, G. 1924. Relations between American and European Tertiary echinoid faunas. *Geological Society of America Bulletins*, 35(4): 827-846.

Toulmin, L.D. 1969. Paleocene and Eocene guide fossils of the eastern Gulf Coast Region. *Transactions Gulf Coast Association of Geological Society*, 19: 465-487.

Toulmin, L.D. 1977. Stratigraphic distribution of Paleocene and Eocene fossils in the Eastern Gulf Coast region. *Geological Survey of Alabama Monographs*, 13: 1-602.

Ward, L.W., Blackwelder, B.W., Gohn, G.S., and Poore, R.Z. 1979. Stratigraphic revision of Eocene, Oligocene and lower Miocene formations of South Carolina. *Geologic Notes, South Carolina Geological Survey*, 23: 2-23.

Zachos, L. G. 2009. The sand dollar *Periarchus lyelli* (Echinoidea: Clypeasteroida: Scutelliformes) in the Caddell Fromation (Upper Eocene) of Texas. *Texas Journal of Science*. V. 61. p. 181-186.

Zachos, L.G., and Molineux, A. 2003. Eocene echinoids of Texas. *Journal of Paleontology*, 77(3): 491-508.

Zullo, V.A., and Harris, W.B. 1987. Sequence stratigraphy, biostratigraphy and correlation of Eocene through lower Miocene strata in North Carolina. *Cushman Foundation for Foramaniferal Research, Special Publications*, 24: 197-213.

SOUTHEASTERN GEOLOGY
V. 49, No. 3, March 2013 p. 133-143

CRINOIDEA FROM THE FORT PAYNE OF NORTH-CENTRAL ALABAMA AND SOUTH-CENTRAL TENNESSEE (PHYLUM ECHINODERMATA; MISSISSIPPIAN)

ELYSSA B. KRIVICICH[1]
elyssa.krivicich@gmail.com

WILLIAM I. AUSICH[1]
ausich.1@osu.edu

Richard G. Keyes[2]
rgeo@bellsouth.net

[1]*School of Earth Sciences,155 South Oval Mall,The Ohio State University,Columbus, OH 43210*
[2]*P.O. Box 21061,Huntsville, AL 35813*

ABSTRACT

New crinoid and blastoid faunas are reported from the Fort Payne Chert of north-central Alabama and the Fort Payne Formation of south-central Tennessee, including 27 crinoid and three blastoid species. One new species, *Magnuscrinus kammeri*, is described. Based on a nearly identical fauna in south-central Kentucky, the Fort Payne Formation in north-central Alabama and south-central Tennessee is late Osagean (early Viséan; Mississippian time bin 6). Thus, throughout the outcrop belt from south-central Kentucky to north-central Alabama, the age is the same. This indicates that the strike of the prograding Fort Payne Chert and Formation was approximately coincident with the present-day outcrop belt.

INTRODUCTION

Fort Payne Formation crinoids were among the first reported in North America (Troost, 1849, 1850a, 1850b; Wood, 1909; Ausich, 2009). These crinoids were collected from the Whites Creek Springs locality (Bassler and Moodey, 1943), presumably near Nashville, Tennessee. The exact provenance of these 19th Century specimens is not known, and no data exist on the details of the stratigraphic context from which these fossils were extracted.

Ausich and Meyer (1988, 1990, 1992, 1994), Ausich et al. (1997), Greb et al. (2008), Meyer and Ausich (1992, 1997, 2009), Meyer et al. (1989, 1992, 1995, 1997), Norris (1990), and Terry (1990) have documented a large crinoid and blastoid fauna from the Fort Payne Formation of the Lake Cumberland region of south-central Kentucky and north-central Tennessee. Lake Cumberland faunas are from a diverse array of deeper-water, cratonic siliciclastic and carbonate facies and are demonstrably late Osagean (early Viséan) in age based on the occurrence of conodonts and crinoids (Ausich and Meyer, 1990; Leslie et al., 1996). As presently understood, this fauna is within Mississippian time bin 6 of Ausich and Kammer (2006) and Kammer and Ausich (2007), and it is age equivalent to the Keokuk Limestone (Illinois, Iowa, and Missouri) and the Edwardsville Formation (Indiana).

The Fort Payne Formation of south-central Kentucky was part of the dynamic Mississippian stratigraphic architecture with two time-transgressive sediment wedges migrating through this region. The Borden Formation prograded through south-central Kentucky during the middle Osagean (Sedimentation Seminar, 1972; Ausich et al., 1979; Matchen and Kammer, 1994; Leslie et al., 1996; Richardson and Ausich, 2004; Khetani and Read, 2002; and others) with the westward-most extent in south-central Kentucky along a northwest-southeast line, the Borden Front, through Adair, Russell, and Wayne counties (Sedimentation Seminar, 1972). The Borden Formation was a deltaic clastic wedge that prograded into the area from

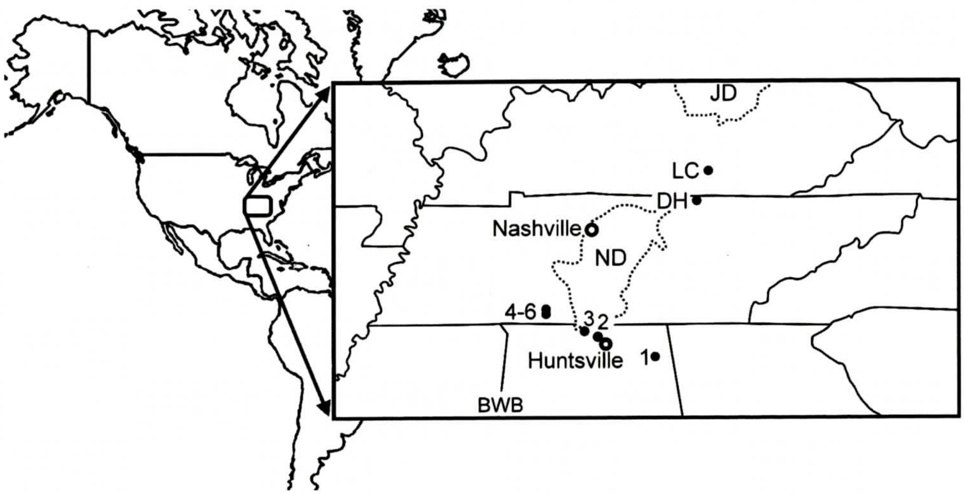

Figure 1– General locality map for sites in north-central Alabama and south-central Tennessee. BWB, Black Warrior Basin; DH, Dale Hollow Lake; JD, Jessamine Dome; LC, Lake Cumberland; ND, Nashville Dome; 1-6 are localities mentioned in the text and in Appendix 1.

the east-northeast. After the cessation of Borden Formation sedimentation, starved basin conditions ensued until the mixed siliciclastic-carbonate deposition of the Fort Payne Formation prograded through south-central Kentucky during the late Osagean.

New, extensive collections of Fort Payne Chert crinoids have been made during the past two decades from north-central Alabama and south-central Tennessee. Herein, we evaluate and compare the composition of the new faunas to those from south-central Kentucky and north-central Tennessee in order to assess the dynamics of Fort Payne Chert/Formation sedimentation at its southern extent.

OCCURRENCES, PRESERVATION, AND MATERIAL

The Fort Payne Chert/Formation is approximately 150 feet (45 m) thick throughout the north-central Alabama and south-central Tennessee outcrop belt. Fresh exposures are generally slightly more than 50% dark gray cherts and light gray limestones. It thins gradually toward the south-southwest to approximately 65 feet (20 m) in the northern part of the Black Warrior Basin (Fig. 1). Toward the south in the vicinity of Birmingham, Alabama, the Fort Payne Formation thins to 10 feet (3 m) (Thomas, 1972). The Fort Payne is deeply weathered in south-central Tennessee and north-central Alabama, and most crinoid occurrences are in glades or at construction sites in which the formation is comprised of clay limestone residuum, chert, and silicified fossils, especially crinoids. Although some stratigraphic relationships may be preserved within the residuum, the lithofacies context is not. The vast majority of specimens have only the outer surface replaced by silica and are complete or partial calyxes. More complete silicification is less common. Isolated calyx plates and numerous columnals and pluricolumnals are also present.

Specimens discussed herein are from several sites in Dekalb, Limestone, and Madison counties Alabama and in Lawrence County, Tennessee (Appendix 1; additional locality data are recorded with the specimens). The most extensive collections are from localities in Lawrence County, Tennessee. Specimens are deposited in the U.S. National Museum, Smithsonian Institution, Washington, D.C. (USNM) and the Orton Geological Museum, The Ohio State University. Locality details are recorded with specimens.

CRINOID FAUNAS

More than 260 crinoid and three blastoid

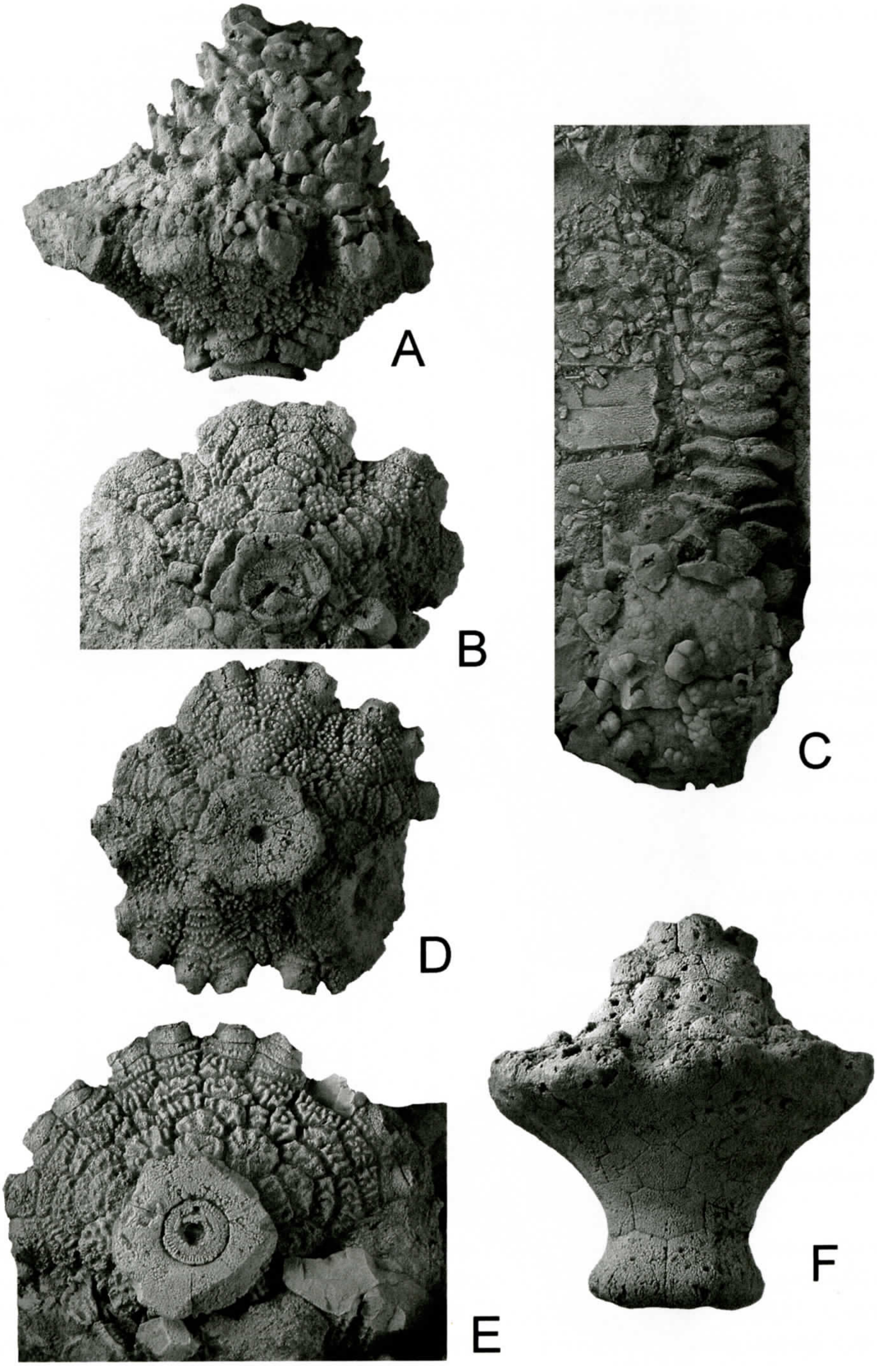

Figure 2– Fort Payne Formation crinoids, X1.5. A, B, *Magnuscrinus kammeri* n. sp., holotype, USNM 546039; A, lateral view of calyx and proximal anal tube; B, basal view of calyx. C, *Magnuscrinus kammeri* n. sp., paratype, USNM 546041, specimen with broken calyx but nearly compete anal tube. D, *Magnuscrinus kammeri* n. sp., paratype, USNM 546040, basal view of calyx. E, *Magnuscrinus kammeri* n. sp., paratype, USNM 546042, basal view of calyx. F, *Uperocrinus nashvillae*, USNM 546044, lateral view of calyx.

Table 1. Relative abundance of crinoids from localities in north-central Alabama and south-central Tennessee. See Fig. 1 and Appendix 1 for locality information.

	Localities						
Species	**1**	**2**	**3**	**4**	**5**	**6**	**Total**
Agaricocrinus americanus	3	2	0	0	49	7	61
Alloprosallocrinus conicus	3	2	1	0	49	3	58
Uperocrinus nashvillae	0	3	2	0	35	7	47
Eretmocrinus magnificus	9	1	0	0	22	5	37
Synbathocrinus swallovi	1	0	0	0	11	2	14
Barycrinus stellatus	0	0	0	0	8	2	10
Gilbertsocrinus tuberosus	0	1	1	0	5	1	8
Uperocrinus robustus	0	0	0	0	5	1	6
Magnuscrinus praegravis	1	0	2	0	3	0	6
Abatocrinus grandis	0	0	1	0	4	0	5
Thinocrinus lowei	0	0	0	0	4	1	5
Barycrinus rhombiferus	0	1	0	0	2	1	4
Catillocrinus tennesseeae	0	0	0	0	4	0	4
Agaricocrinus crassus	0	0	0	0	1	2	3
Cyathocrinites iowensis	0	0	0	0	3	0	3
Gaulocrinus veryi	0	0	0	2	1	0	3
Actinocrinites sp. 1	0	0	0	0	2	0	2
Actinocrinites sp. 2	0	0	0	0	2	0	2
Magnuscrinus kammeri n. sp.	0	0	0	0	2	0	2
Barycrinus spurius	0	0	0	1	0	0	1
Cyathocrinites farleyi	0	0	0	0	1	0	1
Cyathocrinites harrodi	0	0	0	0	1	0	1
Dorycrinus gouldi	0	0	0	0	0	1	1
Eretmocrinus sp.	0	0	0	0	1	0	1
Eucladocrinus millebrachiatus	0	0	0	0	1	0	1
Forebesiocrinus saffordi	0	0	0	0	1	0	1
Methichtyocrinus tiaraeformis	0	0	0	0	1	0	1

specimens were identified from the Fort Payne of north-central Alabama and south-central Tennessee. In total, this fauna contains 27 crinoid species assigned to 18 genera and three blastoid species assigned to three genera. Among these is the new species, *Magnuscrinus kammeri* (Fig. 2A-E). The most abundant crinoids are monobathrid camerate and disparid crinoids, including the camerates *Agaricocrinus americanus* (Roemer, 1852-1854) (Fig. 3A, 3B); *Alloprosallocrinus conicus* Casseday and Lyon, 1862 (Fig. 3E, 3F); *Uperocrinus nashvillae* (Hall, 1858) (Fig. 2F); *Eretmocrinus magnificus* Lyon and Casseday, 1859 (Fig. 3G); and the disparid *Synbathocrinus swallovi* Hall, 1858. These five species make up more than 75% of new specimens from north-central Alabama and south-central Tennessee (Table 1).

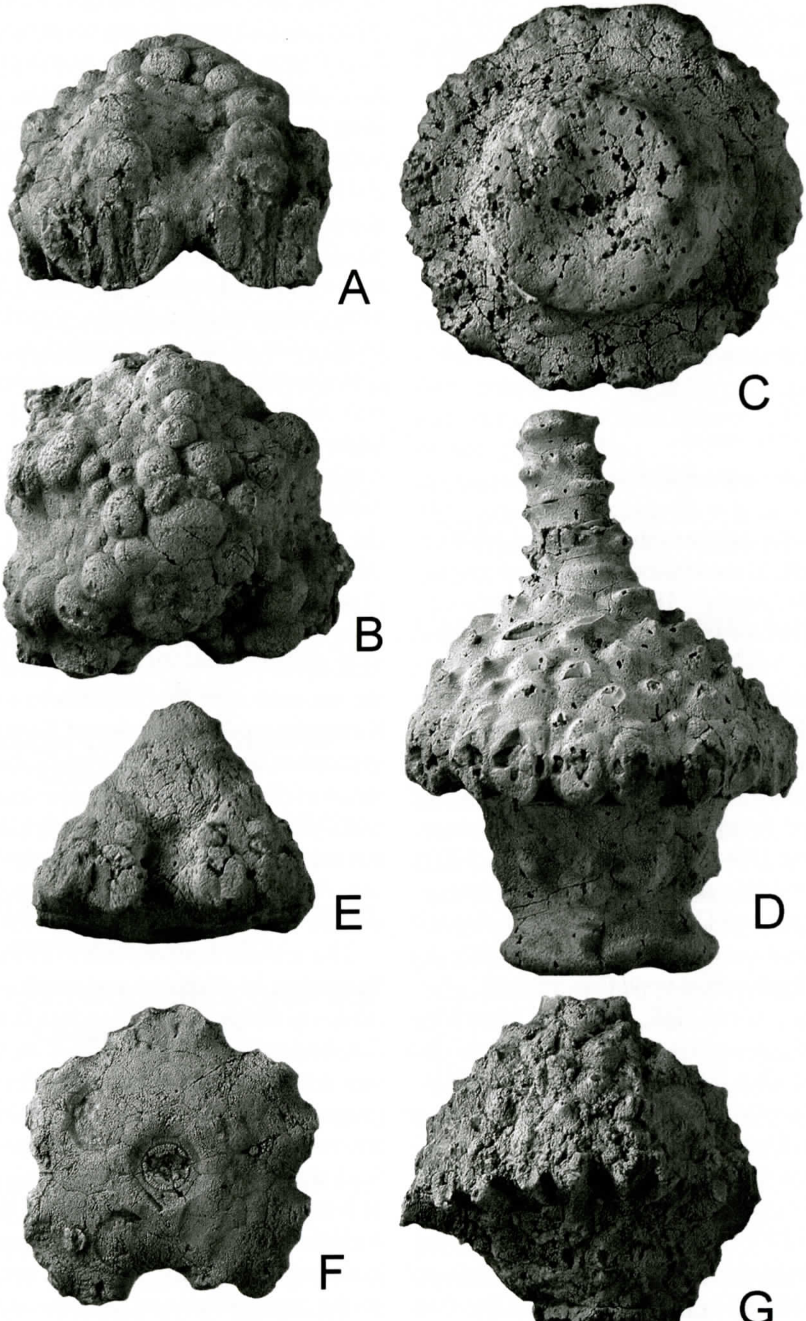

Figure *3*– Fort Payne Formation crinoids, X1.5. A, B, *Agaricocrinus americanus*, USNM 546045; A, lateral view of calyx; B, tegmen view. C, D, *Eretmocrinus* sp., USNM 546048; C, basal view calyx; D, lateral view of calyx. E, F, *Alloprosallocrinus conicus*, USNM 546046; E, lateral view of calyx; F, basal view of calyx. G, *Eretmocrinus magnificus*, USNM 546047, lateral view of calyx.

Table 2. Relative abundance of ten most common crinoids from the Fort Payne Formation in south-central Kentucky and north-central Alabama.

Agaricocrinus americanus
Eretmocrinus magnificus
Alloprosallocrinus conicus
Synbathocrinus swallovi
Halysiocrinus tunicatus
Macrocrinus sp.
Cyathocrinites iowensis
Uperocrinus robustus
Thinocrinus sp.
Uperocrinus nashvillae

The fauna also contains the following additional monobathrid camerates *Abatocrinus grandis* (Lyon and Casseday, 1859); *Actinocrinites* sp. 1; *Actinocrinites* sp. 2; *Agaricocrinus crassus* Wetherby, 1881; *Dorycrinus gouldi* (Hall, 1858); *Eucladocrinus millebrachiatus* Wachsmuth and Springer, 1878 (recognized from isolated columnals); *Magnuscrinus praegravis* (Miller, 1892); *Magnuscrinus kammeri* n. sp.; *Thinocrinus lowei* (Hall, 1858); and *Uperocrinus robustus* (Wachsmuth and Springer, 1897); the diplobathrid camerate *Gilbertsocrinus tuberosus* Lyon and Casseday, 1859; the disparid *Catillocrinus tennesseeae* Shumard, 1865; the flexibles *Gaulocrinus veryi* Rowley, 1903; *Forbesiocrinus saffordi* Hall, 1859; and *Metichthyocrinus tiaraeformis* (Hall, 1858); and the primitive cladids *Barycrinus rhombiferus* (Owen and Shumard, 1852); *Barycrinus spurius* Hall, 1858; *Barycrinus stellatus* Hall, 1858; *Cyathocrinites farleyi* Meek and Worthen, 1866; and *Cyathocrinites harrodi* (Wachsmuth and Springer, 1880) (Table 1). In addition, the blastoids *Deliablastus cumberlandensis* Ausich and Meyer, 1988; *Euryblastus veryi* (Rowley, 1902); and *Granatocrinus granulatus* (Roemer, 1851) were also recovered.

With the exception of one taxon, *C. harrodi*, all species in the north-central Alabama and south-central Tennessee region also occur in the Fort Payne Formation faunas from south-central Kentucky and north-central Tennessee, including the new species of *Magnuscrinus*. Although *C. harrodi* is not recognized from the Fort Payne Formation of south-central Kentucky and north-central Tennessee, it is known from other late Osagean strata in Kentucky and Indiana (Kammer and Ausich, 1996).

Despite taphonomic biases for crinoid preservation that certainly occur in Fort Payne faunas (Meyer et al., 1989), crinoids in the two regions should have experienced broadly the same preservational biases, thereby allowing comparison of relative abundances. Four of the first five most abundant species from north-central Alabama and south-central Tennessee (*Agaricocrinus americanus*, *Alloprosallocrinus conicus*, *Eretmocrinus magnificus*, and *Synbathocrinus swallovi*) (Table 1) correspond to the four most abundant crinoids from south-central Kentucky and north-central Tennessee (Table 2). The fourth most abundant species from north-central Alabama and south-central Tennessee (*Uperocrinus nashvillae*) is among the ten most abundant crinoids in south-central Kentucky and north-central Tennessee. One distinction between these two faunas is the absence of *Halysiocrinus tunicatus* (Hall, 1860) in north-central Alabama and south-central Tennessee. This may represent a facies bias, as the new faunas are from limestone residuum (Ausich and Meyer, 1990), but this is not clear.

The crinoid fauna of the Fort Payne Chert/Formation in Alabama and south-central Tennessee is nearly identical to that from the Lake Cumberland region and, therefore, must represent a contemporaneous episode of Fort Payne progradation. The 27 crinoid species in the Alabama/Tennessee fauna are exclusively known from the late Osagean (Mississippian time bin 6 of Ausich and Kammer, 2006 and Kammer and Ausich, 2007). Further, the two areas must have had similar paleoenvironmental settings, based on the composition and preservation of the faunas.

SYSTEMATIC PALEONTOLOGY

Terminology of the crinoid endoskeleton follows Ubaghs (1978a) with modifications from Ausich et al. (1999). Crinoid orientation is in reference to the oral-aboral axis, following Ubaghs (1978a). With a specimen oriented vertically, height is parallel to the oral-aboral axis (tips of the arms the highest; holdfast the lowest), and width is perpendicular to the oral-aboral axis. Terminology for calyx shapes follows Ubaghs (1978a, fig. 72). Specimens from this study are deposited in the U.S. National Museum of Natural History, Smithsonian Institution, Washington, D.C. (USNM) and in the Ohio State University Orton Geological Museum. All specimen measurements are in mm; * indicates a measured specimen was either incomplete or broken.

CLASS CRINOIDEA J. S. MILLER, 1821

Subclass CAMERATA Wachsmuth and Springer, 1885

Order MONOBATHRIDA Moore and Laudon, 1943

Suborder COMPSOCRININA Ubaghs, 1978b

Superfamily CARPOCRINACEA de Koninck and Le Hon, 1854

Family BATOCRINIDAE Wachsmuth and Springer, 1881

Genus ERETMOCRINUS Lyon and Casseday, 1859

Eretmocrinus sp.

Figure 3C, 3D

Type species: *Eretmocrinus magnificus* Lyon and Casseday, 1859; by monotypy.
Material: USNM 546048.
Remarks: A single, unusual specimen is assigned to *Eretmocrinus* sp. Its morphology is distinct from the common Fort Payne *Eretmocrinus, E. magnificus*. *Eretmocrinus* sp. has a very thick basal ridge, a relatively slight expansion of the calyx wall upward from the basal ridge to the point where fixed brachials begin to flare outward, and arm facets oriented outward. In contrast, *E. magnificus* has a thin basal ridge, a marked expansion upward along the calyx wall, and arm facets oriented outward and upward.

Eretmocrinus magnificus populations have considerable morphologic variability. Also, Ausich and Meyer (1994) argued for hybridization within *Eretmocrinus* (note the two species hypothesized to have crossed are now placed in different genera, Ausich and Kammer, 2010). Thus, additional specimens with the unusual morphology of *Eretmocrinus* sp. are required before a new species can be proposed.
Occurrence: Fort Payne Formation (late Osagean, early Viséan) from Lawrence County, Tennessee (Locality 5).
Measurements: USNM 546048: calyx height, 18.2; calyx distal width, 36.1; basal ridge width, 19.5; tegmen height, 18.7; and anal tube height, 16.4*.

Genus MAGNUSCRINUS Ausich and Kammer, 2010

Type species: *Eretmocrinus yandelli* Shumard, 1858.
Emended Diagnosis: Calyx shape low bowl or flat cone; basal concavity absent; calyx lower than tegmen; calyx plates very nodose or covered with fine nodes; median ray ridges absent; plates commonly with distinct sutures; basal plates low, with large elongate proximal nodes; radial plates low; first primibrachial tetragonal; rays lobate; regular interrays typically in contact with the tegmen (although may be variable on a single specimen); CD interray in contact with tegmen; tegmen low to medium inverted cone; tegmen plates very nodose or spinose; anal tube cylindrical; arm facets face outward (subvertical); and free arms 12-25, other aspects of free arms unknown.
Included species: Five species are recognized in *Magnuscrinus*, including *M. celsus* (Miller and Gurley, 1894), *M. praegravis* (Miller, 1892), *M. spinosus* (Miller and Gurley, 1895), *M. kammeri* n. sp., and *M. yandelli* (Shumard, 1858).

Magnuscrinus kammeri n. sp.

Figure 2A-2E

Material: Holotype: USNM 546039 (locality 5); paratype USNM 546040 (locality 5); paratypes USNM 546041-546043 (Gross Creek West).

Diagnosis: Calyx intermediate height for genus, calyx plate sculpturing of numerous fine nodes, tegmen plate sculpturing with very large nodes.

Description: Calyx size relatively small for genus, flat cone shape (Fig. 3A), base with continuous ridge formed by nodes (Fig. 3D, 3E), shallow basal concavity, arms grouped but not lobate (Fig. 3B), calyx plates with numerous small nodes (Fig. 3B) (may be coalesced into short ridges (Fig. 3E), and plate sutures distinct.

Basals three, wider than high, equal in size, lower than radials. Radials five, hexagonal or heptagonal in shape, wider than high, higher than basals. Primanal hexagonal, larger than radial plates, interrupts radial circlet, second range in the posterior with two much smaller plates; posterior plating P-2-1 or P-2-1-1; posterior interray in contact with tegmen. Normal interrays slightly narrower than CD interray, first interradial 10-sided; plating 1-2, may or may not be in contact with tegmen (Fig. 3B). First primibrachial tetragonal, much wider than high; second primibrachial axillary, pentagonal, slightly larger than first primibrachial, wider than high; first and second secundibrachials approximately the same size as second primibrachials; last fixed brachial second or third tertibrachial (Fig. 3E); arm openings subelliptical, higher than wide, directed obliquely upward.

Tegmen high with straight sides (Fig. 3A), plates with very large nodes; anal tube high and slender, central, plates with large elongate nodes (Fig. 3C). Twenty facets for free arms, other aspects of arms not known. Column unknown.

Remarks: The distinctive calyx plate sculpturing distinguishes *M. kammeri* from other species of *Magnuscrinus*.

Occurrence: Fort Payne Formation (late Osagean, early Viséan) from Lawrence County, Tennessee (Locality 5); and Gross Creek West, Lake Cumberland shoreline, Russell County, Kentucky (Ausich and Meyer, 1988). The former is the type locality.

Measurements: USNM 546039 (holotype): calyx height, 9.3; calyx width, 35.0*, tegmen height, 22.0*. Paratypes: USNM 546040: calyx height, 10.5; calyx width, 31.5; USNM 546041: calyx height, 13.4; calyx width, 34.8; USNM 546043: calyx height, 9.1*; calyx width, 17.5*; anal tube height, 37.2*.

Etymology: This species name recognizes Thomas W. Kammer for his extensive contributions to the study of Mississippian crinoids.

CONCLUSIONS

The Fort Payne Formation is late Osagean (early Viséan; Mississippian time bin 6) throughout the outcrop belt from south-central Kentucky to north-central Alabama, based on nearly identical crinoid and blastoid faunas. This indicates that the strike of the prograding Fort Payne was coincident with the present-day outcrop belt. These data confirm that during the late Osagean, the Fort Payne Chert/Formation was most probably prograding from the southeast to the northwest, as generally assumed. Twenty-seven crinoid species are recorded from the Alabama/Tennessee region, all but one of which occur in the Lake Cumberland region of south-central Kentucky and north-central Tennessee. One new species and one very unusual specimen of *Eretmocrinus* also occur in this fauna. Thus, despite the fact that deep weathering precludes detailed facies analysis, it may be anticipated that facies similar to those of the Lake Cumberland region extended as far south as northern Alabama.

ACKNOWLEDGMENTS

A special thank you to Dorothy Noak; this study would not have been possible without her kindness. L. Gilbert, C. Grisham, and T. and C. Wilburn shared their site information and specimens from north-central Alabama and south-central Tennessee. D.L. Meyer, WIA and their students collected the specimens from the Lake Cumberland Region. We thank D.L. Meyer, University of Cincinnati, for access to specimens. Also S.K. Donovan and T.W. Kammer improved an earlier draft of manuscript. This research was supported in part by the National Science Foundation (EAR-8407516 and EAR-8903486; WIA).

REFERENCES

Ausich, W. I., 2009, A critical evaluation of the status of crinoids studied by Dr. Gerard Troost (1776-1850): Journal of Paleontology, v. 83, p. 484-488.

Ausich, W. I., and Kammer, T. W., 2006, Stratigraphical and geographical distribution of Lower Carboniferous Crinoidea from England and Wales: Proceedings of the Yorkshire Geological Society, v. 56(2), p. 91-109.

Ausich, W. I., and Kammer, T. W, 2010, Generic concepts in the Batocrinidae Wachsmuth and Springer, 1881 (Class Crinoidea): Journal of Paleontology, v. 84, p. 32-50.

Ausich, W. I., and Meyer, D. L., 1988, Blastoids from the late Osagean Fort Payne Formation (Kentucky and Tennessee): Journal of Paleontology, v. 62, p. 269-283.

Ausich, W. I., and Meyer, D. L., 1990, Origin and composition of carbonate buildups and associated facies in the Fort Payne Formation (Lower Mississippian, south-central Kentucky): an intetrated sedimentologic and paleoecologic analysis: Geological Society of America Bulletin, v. 102, p. 129-146.

Ausich, W.I., and Meyer, D. L., 1992, Crinoidea Flexibilia (Echinodermata) from the Fort Payne Formation (Lower Mississippian; Kentucky and Tennessee): Journal of Paleontology, v. 66, p. 825-838.

Ausich, W.I., and Meyer, D. L., 1994, Hybrid crinoids in the fossil record (Early Mississippian, Phylum Echinodermata): Paleobiology, v. 2, p. 362-367.

Ausich, W. I., Kammer, T. W., and Lane, N. G., 1979, Fossil communities of the Borden (Mississippian) delta in Indiana and northern Kentucky: Journal of Paleontology, v. 53, p. 1182-1196.

Ausich, W. I., Kammer, T. W., and Meyer, D. L., 1997, Middle Mississippian disparid crinoids from the midcontinental United States: Journal of Paleontology, v. 71, p. 131-148.

Ausich, W. I., Brett, C. E., Hess, H., and Simms, M. J., 1999, Crinoid form and function, *in* H. Hess, Ausich, W. I., Brett, C. E., and Simms, M. J., Fossil Crinoids, p. 3-30 (Cambridge University Press, Cambridge, U.K.).

Bassler, R. S., and Moodey, M. W., 1943, Bibliographic and faunal index of Paleozoic pelmatozoan echinoderms: Geological Society of America Special Paper, v. 45, 734 p.

Casseday, S. A., and Lyon, S. S., 1862, Description of two new genera and eight new species of fossil Crinoidea from the rocks of Indiana and Kentucky: Proceedings of the American Academy of Arts and Sciences, v. 5, p. 16-31.

Greb, S. F., Potter, P. E., Meyer, D. L., and Ausich, W. I., 2008, Mud mounds, paleoslumps, crinoids and more; the geology of the Fort Payne Formation at Lake Cumberland, south-central Kentucky. Kentucky Geological Survey Field Guide (*www.professionalgeologist.org/guidebook.thtm*).

Hall, J., 1858, Chapter 8. Palaeontology of Iowa. *in* J. Hall, and Whitney, J. D., Report of the Geological Survey of the state of Iowa: Embracing the results of investigations made during portions of the years 1855, 56 &: 57, v. 1, part II; Palaeontology, p. 473-724.

Hall, J., 1859, Contributions to the palaeontology of Iowa, being descriptions of new species of Crinoidea and other fossils. Geological Report of Iowa, Vol. 1 supplement, part 2, 92 p.

Hall, J., 1860, Observations upon a new genus of Crinoidea. *Cheirocrinus, in* Appendix F. Contributions to Palaeontology, 1858 & 1859: Thirteenth Annual Report of the Regents of the University of the State of New York, on the Condition of the State Cabinet of Natural History, and the Historical and Antiquarian Collection Annexed thereto, State of New York in Senate Document 89, p. 121-124.

Kammer, T. W., and Ausich, W. I., 1996, Primitive cladid crinoids from the upper Osagean-lower Meramecian (Mississippian) rocks of the east-central United States: Journal of Paleontology, v. 70, p. 835-866.

Kammer, T. W., and Ausich, W. I., 2007, Stratigraphical and geographical distribution of Mississippian Crinoidea from Scotland: Earth and Environmental Science Transactions of the Royal Society of Edinburgh, v. 98, p. 139-150.

Khetani, A. B., and Reed, J. F., 2002, Sequence development of a mixed carbonate-siliciclastic, high relief ramp, Mississippian, Kentucky, USA: Journal of Sedimentary Research, v. 72, p. 657-672.

Koninck, L. G. de, and Le Hon, H., 1854, Recherches sur les crinoides du terrain carbonifere de la Belgique: Academie Royal de Belgique Memoir, v. 28(3), 215 p.

Leslie, S. A., Ausich, W. I., and Meyer, D. L., 1996, Lower Mississippian sedimentation dynamics and conodont biostratigraphy (lowermost Fort Payne Formation) along the southeastern margin of the Eastern Interior Seaway: Southeastern Geology, v. 36, p. 27-35.

Lyon, S. S., and Casseday, S. A., 1859, Description of nine new species of Crinoidea from the Subcarboniferous rocks of Indiana and Kentucky: American Journal of Science and Arts, series 2, v. 28, p. 233-246.

Matchen, D. L., and Kammer, T. W., 1994, Sequence stratigraphy of the Lower Mississippian Price and Borden Formations in southern West Virginia and eastern Kentucky: Southeastern Geology, 34, p. 25-41.

Meek, F. B., and Worthen, A. H., 1866, Contributions to the palaeontology of Illinois and other western states: Proceedings of the Academy of Natural Sciences of Philadelphia (1865), v. 17, p. 251-274.

Meyer, D. L., and Ausich, W. I., 1992, Fort Payne carbonate facies (Mississippian) of south-central Kentucky: Ohio Geological Society Miscellaneous Report v. 4, Field Trip 14, Annual Meeting of the Geological Society of America, Cincinnati, Ohio, 20 p.

Meyer, D. L., and Ausich, W. I., 1997, Morphologic variation within and among populations of the camerate crinoid *Agaricocrinus* (Lower Mississippian, Kentucky and Tennessee): breaking the spell of the mushroom: Journal of Paleontology, v. 71, p. 896-917.

Meyer, D. L., and Ausich, W. I., 2009, Fort Payne carbonate facies [Mississippian] of south-central Kentucky: Field Guide, 2009 North American Paleontological Convention, 33 p.

Meyer, D. L., Ausich, W. I. and Terry, R. E., 1989, Comparative taphonomy of echinoderms in carbonate facies. Fort Payne Formation (Lower Mississippian) of Kentucky and Tennessee: Palaios, v. 4, p. 533-552.

Meyer, D. L., Ausich, W. I., and Potter, P. E., 1992, Mississippian clinoform: lithologic and paleoecologic diversity amid slopes, slides, and mounds: Palaios, v. 7, p. 335-336.

Meyer, D. L., Ausich, W. I., Bohl, D. T., Norris, W. A., and Potter, P. E., 1995, Carbonate mudmounds in the Fort Payne Formation (Lower Carboniferous), Cumberland saddle region, Kentucky and Tennessee, USA. *in* C. L. V. Monty, Boscence, D. W., Bridges, J. P. H., and Pratt, B. R. (eds.). Carbonate mud mounds, their origin and evolution, p. 273-287 (International Association of Sedimentologists, Special Publications, 23).

Meyer, D. L., Potter, P. E., Theis, J. L., Ausich, W. I., and Leslie, S. A., 1997, A deep to shallow transtition in the Fort Payne Formation (Lower Mississippian) Kentucky Highway 61, Cumberland County, Kentucky: Kentucky Geological Survey, Map and Chart Series, v. 12, Series XI.

Miller, J. S., 1821, A natural history of the Crinoidea, or lily-shaped animals; with observations on the genera, *Asteria, Euryale, Comatula* and *Marsupites*. Bryan & Co., Bristol, England, 150 p.

Miller, S.A., 1892, Palaeontology: Indiana Department of Geology and Natural Resources, 17th Annual Report (1891), p. 611-705.

Miller, S. A., and Gurley, W. F. E., 1894, New genera and species of Echinodermata: Illinois State Museum Bulletin, v. 5, 53 p.

Miller, S. A., and Gurley, W. F. E., 1895, Description of new species of Palaeozoic Echinodermata: Illinois State Museum Bulletin, v. 6, 62 p.

Moore, R. C., and Laudon, L. R., 1943, Evolution and classification of Paleozoic crinoids: Geological Society of America Special Paper, v. 46, 151 p.

Norris, W.A., 1990, Paleoecology and paleocommunity analysis of green shale faunas from the Fort Payne Formation (Lower Mississippian) of south-central Kentucky and north-central Tennessee: Unpublished Masters Thesis, University of Cincinnati, 226 p.

Owen, D. D., and Shumard, B. F., 1852, Descriptions of seven new species of crinoidea from the subcarboniferous of Iowa and Illinois: Journal of the Academy of Natural Sciences of Philadelphia, ser. 2, v. 2, p. 89-94.

Richardson, J. G., and Ausich, W. I., 2004, Miospore biostratigraphy of the Borden Formation (Osagean; Tournaisian/Visean) of Kentucky and Indiana, U.S.A.: Palynology, v. 28, p. 159-174.

Roemer, C.F. 1851. Monographie der fossilen Crinoidenfamilie der Blastoideen und der Gattung *Pentatrematites* im Besonderen. Archive für Naturgeschichte, 17:323-397.

Roemer, C. F., 1852-1854, Erste Periode, Kohlen-Gebirge. *in* Lethaea Geognostica, H. G. Bronn, 1851-1856, 3rd edit., v. 2, p. 1-788, (Echinoderms, p. 210-291) (Stuttgart, E. Schweizerbart).

Rowley, R. R., 1901-1904, Description of fossils: *In* G. K. Green, Contribution to Indiana Palaeontology. New Albany, Indiana, v. 1, no. 7, p. 50-60, pl. 19-21 (1901a); no. 8, p. 62-74, pl. 22-24 (1901b); no. 10, p. 85-97, pl. 28-30 (1902a); no. 11, p. 98-109, pl. 31-33 (1903a); no. 12, p. 110-129, pl. 34-36 (1903b); no. 13, p. 130-137, pl. 37-39 (1903c); no. 14, p. 138-145, pl. 40-42 (1903d); no. 15, p. 146-155, pl. 43-45 (1903e); no. 16, p. 156-167, pl. 46-48 (1903f); no. 17, p. 168-175, pl. 49-51 (1904a); no. 18, p. 176-184, pl. 52-54 (1904b); no. 19, p. 185-197, pl. 55-57 (1904c).

Sedimentation Seminar, 1972, Sedimentology of the Mississippian Knifley Sandstone and Cane Valley Limestone in south-central Kentucky: Kentucky Geological Survey, series X, Report of Investigations v. 13, 30 p.

Shumard, B. F., 1858, Description of new fossil Crinoidea from the Palaeozoic rocks of the western and southern portions of the United States: Transactions of the St. Louis Academy of Science (1857), v. 1, p. 71-80.

Shumard, B. F., 1865-1866, Catalogue of Palaeozoic fossils, Part 1, Echinodermata: Transactions of the St. Louis Academy Science, v. 2, no. 2, p. 334-394 (1865); p. 395-407 (1866).

Terry, R. E., 1990, Echinoderm paleoecology and taphonomy of carbonate debris flows, Fort Payne Formation (Lower Mississippian), Dale Hollow Reservoir, Tennessee: Unpublished Masters Thesis, University of Cincinnati, 180 p.

Thomas, W. A., 1972, Mississippian stratigraphy of Alabama: University of Alabama, Monograph 12, 121 pp.

Troost, G., 1849, Geographical survey of Tennessee: American Journal of Science, series 2, v. 8, p. 419-420.

Troost, G., 1850a, A list of the fossil crinoids of Tennessee: American Association for the Advancement of Science, Proceedings (1849), series 2, v. 8, p. 59-64.

Troost, G., 1850b, Monograph on crinoids discovered in the state of Tennessee. Unpublished, 95 p.

Ubaghs, G., 1978a, Skeletal morphology of fossil crinoids. *in*, R. C. Moore and Teichert, K. (eds.). Treatise on Invertebrate Paleontology, Echinodermata, Pt. T(2), p. T58-T216 (Geological Society of America and University of Kansas Press, Boulder and Lawrence).

Ubaghs, G., 1978b, Camerata, p. T408-T518 *in*, R. C. Moore and Teichert, K. (eds.). Treatise on Invertebrate Paleontology, Echinodermata, Pt. T(2), p. T408-T518 (Geological Society of America and University of Kansas Press, Boulder and Lawrence).

Wachsmuth, C., and Springer, F., 1878, Transition-forms in crinoids and descriptions of 5 new species: Proceedings of the Academy of Natural Sciences of Philadelphia, v. 29, p. 224-266.

Wachsmuth, C., and Springer, F., 1880-1886, Revision of the Palaeocrinoidea: Proceedings of the Academy of Natural Sciences of Philadelphia, Pt. I. The families Ichthyocrinidae and Cyathocrinidae (1880): p. 226-378, (separate repaged p. 1-153); Pt. II. Family Sphaeroidocrinidae, with the sub-families Platycrinidae, Rhodocrinidae, and Actinocrinidae (1881): p. 177-411 (separate repaged, p. 1-237); Pt. III, Sec. 1. Discussion of the classification and relations of the brachiate crinoids, and conclusion of the generic descriptions (1885), p. 225-364 (separate repaged, p. 1-138); Pt. III, Sec. 2. Discussion of the classification and relations of the brachiate crinoids, and conclusion of the generic descriptions (1886), p. 64-226 (separate repaged to continue with section 1, p. 139-302).

Wachsmuth, C., and Springer, F., 1897, The North American Crinoidea Camerata: Harvard College Museum of Comparative Zoology Memoir, v. 20 and 21, 897 p.

Wetherby, A. G., 1881, Descriptions of new fossils from the Lower Silurian and sub-Carboniferous rocks of Kentucky: Journal of the Cincinnati Society of Natural History, v. 4, p.177-179.

Wood, E., 1909, A critical summary of Troost's unpublished manuscript on the crinoids of Tennessee: U.S. National Museum Bulletin, v. 64, 150 p.

APPENDIX 1

Locality 1: Large chert pit in fold belt near Fort Payne, DeKalb County, Alabama; 34° 29.696'N 85° 40.789'W. Currently abandoned and somewhat overgrown.

Locality 2: A short section along a creek near Monrovia, Madison County, Alabama, northwest-west of Huntsville; 34° 47.433'N 86° 42.702'W.

Locality 3: Low roadcut along a county road near Salem, northwestern Limestone County, Alabama; 34° 56.213'N 87° 7.817'W.

Locality 4: Old roadcut north of Iron City, Lawrence Co., Tennessee on County Highway 242, 35° 4.241'N 87° 34.669'W.

Locality 5: Old roadcut along county road in Lawrence County, Tennessee; mostly overgrown.

Locality 6: Hillside on edge of farm field, Lawrence County, Tennessee; mostly overgrown.